

Online Scheduling for LLM Inference with KV Cache Constraints

Patrick Jaillet* Jiashuo Jiang[†] Konstantina Mellou[‡] Marco Molinaro[§]
 Chara Podimata[¶] Zijie Zhou^{||}

Abstract

Large Language Model (LLM) inference, where a trained model generates text one word at a time in response to user prompts, is a computationally intensive process requiring efficient scheduling to optimize latency and resource utilization. A key challenge in LLM inference is the management of the Key-Value (KV) cache, which reduces redundant computations but introduces memory constraints. In this work, we model LLM inference with KV cache constraints theoretically and propose a novel batching and scheduling algorithm that minimizes inference latency while effectively managing the KV cache’s memory.

More specifically, we make the following contributions. First, to evaluate the performance of online algorithms for scheduling in LLM inference, we introduce a hindsight optimal benchmark, formulated as an integer program that computes the minimum total inference latency under full future information. Second, we prove that no deterministic online algorithm can achieve a constant competitive ratio when the arrival process is arbitrary. Third, motivated by the computational intractability of solving the integer program at scale, we propose a polynomial-time online scheduling algorithm and show that under certain conditions it can achieve a *constant* competitive ratio. We also demonstrate our algorithm’s strong empirical performance by comparing it to the hindsight optimal in a synthetic dataset. Finally, we conduct empirical evaluations on a real-world public LLM inference dataset, simulating the Llama2-70B model on A100 GPUs, and show that our algorithm significantly outperforms the benchmark algorithms. Overall, our results offer a path toward more sustainable and cost-effective LLM deployment.

1 Introduction

Large Language Models (LLMs) [Brown et al., 2020, Chowdhery et al., 2023, OpenAI, 2023, Kaplan et al., 2020, Wei et al., 2022] represent a significant advancement in AI, enabling machines to generate human-like text across various languages and contexts. Trained on vast datasets, these models are becoming critical for applications such as chatbots [Anthropic, 2023, Character, 2021, OpenAI, 2019, 2023], search engines [Microsoft, 2023, Google, 2023, Komo, 2023, Perplexity, 2022,

*Department of Electrical Engineering and Computer Science, Massachusetts Institute of Technology. Email: jaillet@mit.edu.

[†]HKUST. Email: jsjiang@ust.hk.

[‡]Microsoft Research. Email: kmellou@microsoft.com.

[§]Microsoft Research. Email: mmolinaro@microsoft.com.

[¶]Sloan School of Management, Massachusetts Institute of Technology. Email: podimata@mit.edu.

^{||}Operations Research Center, Massachusetts Institute of Technology. Email: zhou98@mit.edu. Part of this work was done during a summer internship at Microsoft Research – Redmond.

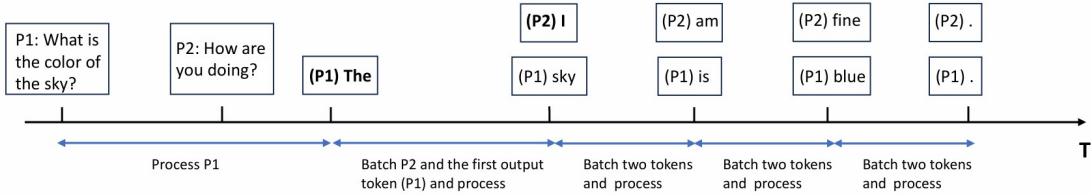


Figure 1: Example of online batching and scheduling.

[You.com, 2020](#)], code assistants [[Amazon, 2023](#), [GitHub, 2021](#), [Replit, 2018](#)], and healthcare services [[Cascella et al., 2023](#), [Peng et al., 2023](#), [Sallam, 2023](#)].

LLM Inference and the KV Cache. LLMs pose substantial computational challenges, particularly during the inference process where inputs are processed to generate responses. In LLM inference, a “*prompt*” is the input text provided to initiate a model’s response generation. These prompts are broken down into smaller units called “*tokens*”, which may consist of words, sub-words, or punctuation marks based on the model’s vocabulary. For instance, the prompt “What color is the sky?” can be tokenized into six units: “What,” “color,” “is,” “the,” “sky,” and “?”. Similarly, a response like “The color is blue.” would be divided into five tokens: “The,” “color,” “is,” “blue,” and “.”. When a prompt request is processed, typically it is not answered all-at-once, and instead it requires multiples rounds of processing to generate the tokens of the answer sequentially; in the previous example, the output token “blue” can only be generated after the preceding one “is” is produced by the model.

Each token is associated with two vectors: the **Key (K)**, which represents the token’s significance to other tokens in determining its relevance, and the **Value (V)**, which stores information that is used in the output if the token is deemed relevant. These KV pairs are computed based *only* on the token content and its absolute position, and once computed, they remain fixed throughout the process.

During inference, the Transformer attention mechanism [[Vaswani et al., 2017](#)] uses the stored keys and values to determine how tokens relate to one another. Without optimization, generating each new token would require recalculating the attention scores over all previously seen tokens, leading to a quadratic increase in computation as the sequence grows. To avoid this, modern LLMs use a *KV cache*, which stores all previously computed keys and values. This allows the model to reuse past computations efficiently, reducing the cost of generating each token to linear in the sequence length. However, the KV cache causes memory usage to grow linearly with the number of tokens, and unmanaged growth can result in the GPU running out of memory [[Hooper et al., 2024](#), [Kang et al., 2024](#)].

Put together, there are three unique challenges posed by LLM inference: (i) each token can only be generated after its predecessor; (ii) the memory usage grows linearly during inference; and (iii) given the scale of real-world LLM inference, decisions must be made within milliseconds, thus making linear or mixed-integer programming solutions unusable.

Batching and Scheduling. When multiple prompt requests are in the queue, batching requests together (rather than handling them one-by-one) and scheduling their processing improves GPU

efficiency. For example, Figure 1 illustrates the online batching and scheduling process for two distinct prompts, P1 (“What color is the sky?”) and P2 (“How are you doing?”), during LLM inference. Initially, P1 is processed within its own batch. When P2 arrives, it must wait, as simultaneous processing of prompts is limited by worker availability. Once P1 is processed and generates its first output token, “The,” the worker batches this token from P1 and the prompt P2 together and processes them together. After P2 produces its first output token, “I”, and P1 produces the next token “sky”, both tokens, “sky” and “I”, are then batched together for efficient token processing, facilitating the subsequent generation of “is” for P1 and “am” for P2.

Our focus. Our focus in this work is to provide *scheduling* algorithms for LLM inference. Scheduling for LLM inference differs from classical scheduling problems primarily because of the bottlenecks introduced by the KV cache (i.e., the linear memory usage growth, and the KV cache’s dynamic behavior).

Importance. Beyond its theoretical importance, optimizing the scheduling policy in LLM inference is crucial in practice for three reasons. First, it can lead to reduced operational costs; the average daily cost of LLM inference for platforms like ChatGPT is approximately \$700,000 [Gil-Press, 2024, Sun, 2023]. Second, it can enhance user satisfaction by minimizing response times. Last but not least, more efficient scheduling promotes sustainability, as LLM inference currently uses vast amounts of electricity and water daily [Gordon, 2024]. For example, ChatGPT’s daily electricity usage exceeds half a million kilowatt-hours (equivalent to the energy consumption of nearly 180,000 U.S. households) and a single conversation uses approximately fifty centiliters of water, akin to the volume of a standard plastic bottle. By optimizing the scheduling policy, we can reduce the number of GPUs required, conserving resources and contributing to sustainability efforts.

1.1 Results Roadmap

In this work, we make the following contributions.

Mathematical model for online batching and scheduling in LLM inference. While many studies have focused on improving LLM inference efficiency via engineering [Agrawal et al., 2023, Kwon et al., 2023, Patel et al., 2023, Pope et al., 2023, Sheng et al., 2023, Yu et al., 2022, Zhong et al., 2024], there is a lack of formal models in this space. To address this gap, we propose a model (Section 2) for optimizing the batching and scheduling policy in LLM inference. *Batching* entails selecting which requests to process concurrently, while *scheduling* determines their timing.

Hindsight optimal benchmark via Integer Programming (IP). In Section 3, we introduce a hindsight optimal benchmark that assumes complete knowledge of future request arrivals and output lengths. We formulate this as an IP that computes the globally optimal scheduling policy minimizing total end-to-end latency under GPU memory constraints. Our IP captures operational constraints, including non-preemptive execution, per-token memory growth, and memory limits. This optimization benchmark serves as a gold standard for evaluating the quality of online scheduling algorithms.

Online batching and scheduling algorithm. In Section 4, we propose a practical online batching and scheduling algorithm: Memory Constrained Shortest First (MC-SF). The algorithm

prioritizes partially completed requests to reduce latency, and then selects additional waiting requests to fill each batch by maximizing batch size while respecting KV cache memory constraints throughout token generation. We characterize feasibility by introducing constraints that anticipate future KV cache memory usage, ensuring that the algorithm only schedules batches that remain within memory limits throughout their execution. While we prove that no deterministic online algorithm can in general have bounded *competitive ratio*, we show that under certain conditions, our proposed algorithm has *constant* competitive ratio, providing theoretical underpinning for its practical performance.

Synthetic-data experiments. In Section 5.1, we conduct numerical experiments on synthetically generated instances to evaluate the performance of our proposed MC-SF relative to the hindsight optimal. We design two arrival models to disentangle the sources of performance loss: one where all requests arrive at time zero (eliminating information asymmetry), and one with online stochastic arrivals (reflecting real-world uncertainty). In the first model, MC-SF has nearly optimal performance, with an average latency ratio of 1.005 and *exact* optimality in 114 out of 200 instances. In the second model, where future arrivals are unknown, the average ratio remains competitive at 1.047.

Experiments on public conversation dataset. In Section 5.2, we perform numerical simulations using the conversation dataset from Zheng et al. [2023], collected from over 210,000 unique IP addresses via the Vicuna demo and Chatbot Arena website. We evaluate our algorithm against benchmark parametrized algorithms with six parameter configurations in both high- and low-demand settings. In both the high- and low- demand settings, our algorithm significantly outperforms the benchmark algorithms. These gains can be translated to reduced energy consumption and lower costs, supporting more sustainable and efficient LLM deployment.

1.2 Other Related Work

Online Scheduling. In online scheduling, a decision-maker needs to decide the optimal timing for job processing as jobs arrive sequentially. There is a large literature in this subject, where different objectives and input models have been studied; see the books/surveys Albers [2003, 2009], Roughgarden [2020], Leung [2004]. A particularly relevant set of studies are those that extend beyond processing individual jobs, where jobs of the same type can be grouped into batches and processed simultaneously [Lucier et al., 2013, Im and Moseley, 2013, Liu and Lu, 2015, Li et al., 2020]. Another relevant line of work considers precedence constraints, either within parts of the requests or between different requests Garg et al. [2019], Azar and Epstein [2002], Robert and Schabanel [2008], Agrawal et al. [2016]. Yet, the unique demands of LLM inference, in particular the growing memory usage in the KV cache and the combination of both batching and the dynamics of sequential token generation, limit the applicability of the existing algorithms.

LLM Inference. LLM inference is a developing field, and, to date, mathematical approaches for optimizing LLM inference remain underexplored. However, numerous engineering-oriented studies are emerging within systems research. For instance, in scheduling, Patel et al. [2023], Zhong et al. [2024] proposed to use separate GPUs for processing only the prompt and the token phases of a request. Regarding batching, works like Yu et al. [2022], Agrawal et al. [2023, 2024b] examine methods for statically or dynamically grouping pending requests for batch execution. Liu et al.

[2024] boosts LLM inference efficiency by introducing multi-head latent attention, which reduces the KV cache through low-rank key-value joint compression. Zhu et al. [2023] proposed approximate caching and dynamic choice of model size to accelerate LLM inference.

2 Model

We study a batching and scheduling problem within a discrete time horizon for a single computational worker (GPU). The worker has a memory constraint $M > 0$.¹ Let \mathcal{I} denote the instance consisting of unprocessed prompt requests arriving over the discrete time horizon. Each request $i \in \mathcal{I}$ has an associated size s_i , representing the number of tokens in the prompt, and response length o_i , indicating the number of tokens in its response. We assume that o_i can be accurately predicted upon the arrival of request i .²

Request Processing. Each request is processed online and undergoes two primary phases:

1. *Prompt Phase:* The prompt is processed in order to generate the initial output token. During this phase, the memory required for request i is s_i , accounting for the storage of key and value matrix for all tokens in the prompt within the KV cache.
2. *Token Phase:* Subsequent tokens are produced sequentially. In this phase, the memory needed to process the j th token of request i ($j \in \{1, 2, \dots, o_i\}$) is $s_i + j$. This increment accounts for each new token’s key and value, which adds 1 to the existing KV cache memory. Consequently, the peak memory usage for processing the final token of request i reaches $s_i + o_i$. After the completion of the last token, the KV cache clears all related memory usage $s_i + o_i$ for that request.

Batch Processing. A batch may include any unprocessed prompt or output token of different requests; when a prompt request is processed in a batch, its first output token is generated, and, similarly, processing an output token results in the generation of the subsequent token upon batch completion. We assume each batch’s processing time is one unit of time, and only one batch can be processed at a time. Moreover, we assume that this process is non-preemptive, meaning that once a prompt request i is added to a batch, it must be processed continuously for o_i periods until its final output token is processed. The memory constraint ensures that for all ongoing requests (those not fully processed or pending final output tokens), the total memory usage at any given moment does not exceed M , i.e., if $S^{(t)}$ is the set of ongoing requests at time t and $o_i^{(t)}$ is the index of the output token of such request i , then it holds that $\sum_{i \in S^{(t)}} (s_i + o_i^{(t)}) \leq M$. The scheduler’s task is to decide when (i.e., in which batch) to start processing each incoming request.

Prompt Arrival Process. In this paper, we consider an online arrival model in which unprocessed prompt requests are assigned to the scheduler sequentially over time. An instance \mathcal{I} consists of prompt requests that arrive one by one, where each request i is associated with an arrival time a_i ; the arrival time a_i , as well as the request sizes (s_i, o_i) are revealed only at the moment when request i arrives. At any time t , the decision-maker has complete knowledge of (a_i, s_i, o_i) for all requests i such that $a_i \leq t$, and no information about requests with $a_i > t$, which have not yet arrived.

¹ M depends on the memory of the GPU and the complexity of the large language model in use.

²Methods for high-accuracy prediction are introduced in Section A.1. In the state-of-the-art approach, the prediction is accurate up to 80% [Zheng et al., 2024].

Evaluation Metrics. We evaluate an algorithm \mathcal{A} 's performance through its *end-to-end latency*. For each request i , its end-to-end latency is computed as $c_i(\mathcal{A}) - a_i$, where $c_i(\mathcal{A})$ is the time the last output token for request i is processed and a_i is the time that request i arrives. We use $\text{TEL}(\mathcal{I}; \mathcal{A}) := \sum_{i \in [n]} c_i(\mathcal{A}) - a_i$ to denote the total end-to-end latency of algorithm \mathcal{A} for a request sequence \mathcal{I} .

3 Hindsight Optimal Benchmark and Integer Programming

To evaluate the performance of an online scheduling algorithm, we introduce a natural benchmark known as the *hindsight optimal*. This benchmark represents an idealized scheduling policy that has complete foresight, i.e., it knows all future request arrivals a_i 's and their corresponding prompt and output lengths s_i and o_i at the start of the time horizon. Although such information is not available to any real-world system, the hindsight optimal serves as a gold standard: it represents the best possible performance that any algorithm could achieve given perfect future knowledge.

Define \bar{T} as an upper bound on the time when all jobs are completed; for instance, we can take $\bar{T} = \sum_{i \in [n]} (a_i + o_i)$. We formulate an Integer Program that computes the minimum possible total end-to-end latency achievable by any scheduling policy:

$$\min \sum_{i \in [n]} \left(\sum_{t=\{a_i, \dots, \bar{T}\}} t \cdot x_{i,t} + o_i - a_i \right) \quad (1)$$

$$\text{s.t.} \quad \sum_{t=\{a_i, \dots, \bar{T}\}} x_{i,t} = 1, \quad \forall i \in [n] \quad (2)$$

$$\sum_{i=1}^n \sum_{k=\max\{a_i, t-o_i\}}^{t-1} (s_i + t - k)x_{i,k} \leq M, \quad \forall t \in [\bar{T}] \quad (3)$$

$$x_{i,t} \in \{0, 1\}, \quad \forall i \in [n], \forall t \in [\bar{T}] \quad (4)$$

In this formulation, the only decision variable is $x_{i,t} \in \{0, 1\}$, which indicates whether request i begins processing at time t . Since the system operates under a non-preemptive scheduling regime, each request i must be processed without interruption for o_i consecutive rounds once it starts. The objective function (1) minimizes the total end-to-end latency over all requests. For each request i , the latency is defined as the time of its last token completion minus its arrival time, i.e., $(t + o_i) - a_i$, if the request starts processing at time t . This is equivalent to minimizing $\sum_{t=a_i}^{\bar{T}} t \cdot x_{i,t} + o_i - a_i$ across all i , where $x_{i,t}$ determines the start time.

Constraint (2) ensures that each request is scheduled exactly once after its arrival. Constraint (3) enforces the GPU memory limit M at each time step t , by summing over the memory usage of all requests that are active at that time. Specifically, a request i , if scheduled to start at time k , will be active at time t for $k + 1 \leq t \leq k + o_i$, which is equivalent to $k \in [t - o_i, t - 1]$. Moreover, since i cannot be scheduled before its arrival time a_i , we have $k \in [\max\{a_i, t - o_i\}, t - 1]$. If request i starts at time k , then it contributes to memory usage at time $t \in [k, k + o_i]$ with an amount equal to $s_i + t - k$, reflecting both the prompt memory s_i and the token-wise KV cache growth over time. Lastly, constraint (4) enforces the binary nature of the scheduling decisions.

This integer program provides an exact characterization of the optimal non-preemptive scheduling policy under complete future information. It jointly captures the timing, memory, and latency structure of the system while remaining compact and interpretable. As such, it serves as a principled hindsight benchmark for evaluating the performance of online algorithms under both stochastic and adversarial arrival models.

4 Efficient Batching and Scheduling Algorithm and Theoretical Results

In this section, we consider the online arrival model described in Section 2, under an adversarial setting where the number of arrivals, the arrival time and size of each prompt, and the output lengths are all chosen by an adversary.

We start by establishing a hardness result for this general online problem. The standard metric for evaluating the performance of an online algorithm is the *competitive ratio*: an algorithm \mathcal{A} has *competitive ratio* α if for every instance \mathcal{I} , the algorithm’s latency $\text{TEL}(\mathcal{I}; \mathcal{A})$ is at most α times that of the hindsight-optimal solution $\text{OPT}(\mathcal{I})$.

We show that no deterministic online algorithm can achieve a competitive ratio better than order \sqrt{n} , i.e., in the worst-case, the gap between any algorithm and the optimal solution needs to grow with the number of requests. The proof of Theorem 4.1 can be found in Appendix B.

Theorem 4.1. *Every deterministic algorithm has a competitive ratio at least $\Omega(\sqrt{n})$.*

Despite this result showing that no deterministic algorithm can guarantee good performance under arbitrary arrival sequences, we now propose a scheduling algorithm for this online problem and demonstrate its effectiveness across a wide range of arrival instances, via both theoretical analysis (below) and numerical experiments (Section 5.1).

Algorithm MC-SF. At each round t , let $R^{(t)}$ represent the set of all requests that have not yet been processed, while $S^{(t)}$ denotes the set of requests that are currently in progress but not yet completed (i.e., some output tokens have been generated, but not all of them). Our algorithm prioritizes processing requests in $S^{(t)}$ first. After processing all the requests currently in $S^{(t)}$, there may still be unused memory in the KV cache, so our algorithm chooses a subset of requests, $U^{(t)} \subset R^{(t)}$ to add to the batch in order to maximize memory utilization and minimize total latency. To be more precise, our algorithm tries to process as many requests as possible within each batch; for that, it aims to maximize the number of requests in $U^{(t)}$, provided that they satisfy memory constraints.

Specifically, for a subset $U \subset R^{(t)}$, let $t_{\max}(U) := \max_{i \in U} \{t + o_i\}$ represent the maximum completion time for all requests in U if they are added to the batch at time t . To ensure U is feasible, the KV cache memory limit must not be exceeded at any $t' \in [t + 1, t_{\max}(U)]$. This requires that:

$$\sum_{i \in S^{(t)}} (s_i + t' - p_i) \cdot \mathbb{1}_{\{o_i \geq t' - p_i\}} + \sum_{i \in U} (s_i + t' - t) \cdot \mathbb{1}_{\{o_i \geq t' - t\}} \leq M, \quad \forall t' \in [t + 1, t_{\max}(U)] \quad (5)$$

where p_i is the starting time to process request i . The first sum accounts for memory usage from ongoing requests in $S^{(t)}$, while the second captures new requests in U . As long as this inequality

is satisfied for all $t' \in [t + 1, t_{\max}(U)]$, U is feasible to add to the batch. Thus, our selection rule is the following: 1) We sort the set of waiting requests $R^{(t)}$ in non-decreasing order of o_i 's, and 2) select the largest prefix that satisfies the allowed memory usage imposed by inequality (5):

$$U^{(t)} = \operatorname{argmax}_{U \text{ prefix of } R^{(t)} \text{ sorted by } o_i\text{'s}} \{ |U| : \text{inequality (5) is satisfied } \forall t' \in [t + 1, t_{\max}(U)] \} \quad (6)$$

We prioritize adding requests with smaller o_i values, as these requests complete more quickly. Additionally, the peak memory usage of each request is $s_i + o_i$. In practice, prompts processed by a single worker tend to have similar input sizes s_i , with relatively low variance, while the output length o_i exhibits greater variability due to the stochastic nature of response generation. As a result, o_i plays a more critical role in determining memory usage, and selecting requests with smaller o_i values typically reduces peak memory consumption, enabling more requests to be packed into each batch. We continue adding requests in this order, checking the feasibility condition of inequality (5). Importantly, we only need to check this constraint at the *completion times* of ongoing or new requests, specifically $p_j + o_j$ for $j \in S^{(t)} \cup U^{(t)}$. This is because (i) memory usage potentially peaks at these completion times, as a request's memory demand increases until it finishes, and (ii) since memory usage varies linearly between start and end times, satisfying the constraint at these peak points ensures feasibility throughout the interval. The complete algorithm is detailed in Algorithm 1. Since this algorithm adds requests to each batch in a shortest-first manner while smartly checking memory constraints over the near future, we refer to it as Memory-Constrained Shortest-First (MC-SF).

Algorithm 1: Memory Constrained Shortest First (MC-SF)

for each round $t = 1$ to T **do**

Let $S^{(t)}$ be the set of requests that have already started processing and $R^{(t)}$ be the remaining (waiting) requests at time t . Set $U^{(t)} = \emptyset$

for each request $i \in R^{(t)}$ in ascending order of o_i **do**

Set a time list $t' = p_j + o_j$ for $j \in S^{(t)} \cup U^{(t)} \cup \{i\}$

if all inequalities in Equation (5) hold for all t' **then**

Add request i to $U^{(t)}$

else

Break the **for** loop

Process the requests in $S^{(t)} \cup U^{(t)}$

The following proposition states that the computational complexity of each round of MC-SF is actually independent of the number of requests, and the proof can be found in Appendix B.

Proposition 4.2. *Given that the memory limit of the KV cache is M , MC-SF has a computational complexity of $O(M^2)$ at each round $t \in [T]$.*

Next, we analyze a special case in which all prompts have identical size $s_i = s$ and arrive simultaneously at time $t = 0$. Under this setting, we show that MC-SF achieves a constant competitive ratio. This case is motivated by practical scenarios where prompt size variation is small and demand is high—meaning many requests are typically waiting to be processed at any given time.

Theorem 4.3. *Consider instances where all requests arrive at time 0 and have the same prompt size. The algorithm MC-SF is $O(1)$ -competitive for such instances, as long as the memory available M is at least twice the maximum memory occupation of a single request in the instance.*

Moreover, if additionally all requests have identical output lengths o , then the competitive ratio of MC-SF is at most 4.

Proof of Theorem 4.3. We prove the first part of the theorem, namely that when all requests come at time 0 and all prompt sizes s_i are identical, then MC-SF is $O(1)$ -competitive. We remark that we have not optimized the constants in the $O(1)$, and opted to prioritize simplicity of exposition.

Fix throughout an instance satisfying the assumption of the theorem. Without chance of confusion, we also use MC-SF to denote the total latency of this algorithm. Also recall that OPT is the latency of the optimal solution in hindsight.

For an output length size o , let n_o be the number of requests in the instance with this output length. Also, let $\text{vol}_o := s \cdot o + \frac{o \cdot (o+1)}{2}$ denote the volume of memory that a request of this output length o occupies; the first summand ($s \cdot o$) is because the input tokens s have to stay in the memory until the end of the processing, and the second term is the memory occupied every time that one more token is process until the total o tokens (i.e., $\sum_{j \in [o]} j$ tokens in the memory). We will bound the total latency of MC-SF and OPT based on these quantities.

Upper bound on the total latency of MC-SF.

Lemma 4.4 (UB on MC-SF). *The total latency incurred by the algorithm MC-SF is at most*

$$\frac{1536}{M} \sum_o n_o \cdot \sum_{o' \leq o} n_{o'} \cdot \text{vol}_{o'} + 24 \sum_o n_o \cdot o$$

To prove this lemma, we will group the possible output lengths $1, \dots, o_{\max}$ in powers of 2. More precisely, let U_ℓ for $\ell = 0, \dots, \lfloor \log o_{\max} \rfloor$ denote the set of requests that have output length in the interval $[2^\ell, 2^{\ell+1})$. Slightly abusing notation, let $\text{vol}_\ell(I)$ be the total amount of memory that the requests U_ℓ occupy in MC-SF's schedule added up over all times in the interval I .

Lemma 4.5. *Consider one of the sets of requests U_ℓ , and let $\underline{o}_\ell := 2^\ell$ and $\bar{o}_\ell := 2^{\ell+1} - 1$ denote the smallest and largest possible output length for requests in this set. Let \underline{t} and \bar{t} be the first and last time the algorithm MC-SF processes a request in U_ℓ . Then the distance between these times can be upper bounded as*

$$\bar{t} - \underline{t} \leq \frac{192}{M} \cdot \sum_{o=\underline{o}_\ell}^{\bar{o}_\ell} n_o \cdot \text{vol}_o + 5\bar{o}_\ell.$$

Proof. (For the remainder of the proof we omit the subscript ℓ in \underline{o}_ℓ and \bar{o}_ℓ .) To prove this, let us partition the interval $\{\underline{t}, \dots, \bar{t}\}$ into disjoint subintervals I_1, I_2, \dots, I_w of length \bar{o} (where I_w is the only exceptional interval that can be smaller than \bar{o}). For an interval $I \subseteq [T]$, let $\text{peak}(I)$ be the peak memory use by MC-SF during this interval. The next lemma essentially says that if the peak memory utilization of an interval I_{j+1} is large, then the total volume of requests in U_ℓ scheduled “around” that point has to also be large.

Claim 4.6 (Peak to volume). Consider any 3 consecutive intervals I_j, I_{j+1}, I_{j+2} of length \bar{o} . Then $\text{vol}_\ell(I_j \cup I_{j+1} \cup I_{j+2}) \geq \frac{1}{4} \text{peak}(I_{j+1}) \cdot \frac{\text{vol}_\ell}{s + \bar{o}}$.

Proof of Claim 4.6. Let $\tilde{t} \in I_{j+1}$ be the time when the peak memory occupation $\text{peak}(I_{j+1})$ happens. Since the interval I_{j+1} is strictly between times \underline{t} and \bar{t} , by definition of the algorithm it only processes requests of U_ℓ (i.e., with output lengths between $2^\ell = \underline{o}$ and $2^{\ell+1} - 1 = \bar{o}$ in I_{j+1}), and so only those contribute to the memory occupation at time \tilde{t} . If k of these requests contribute to this peak occupation, then each contributes at most $s + \bar{o}$ to it; thus, we have $k \geq \frac{\text{peak}(I_{j+1})}{s + \bar{o}}$. Each such request is completely contained in the bigger interval $I_j \cup I_{j+1} \cup I_{j+2}$, each such request contributes with at least $\text{vol}_\underline{o}$ to the memory volume $\text{vol}_\ell(I_j \cup I_{j+1} \cup I_{j+2})$, which then gives $\text{vol}_\ell(I_j \cup I_{j+1} \cup I_{j+2}) \geq k \cdot \text{vol}_\underline{o}$. Finally, since $\underline{o} \geq \frac{1}{2}\bar{o}$, a quick calculation shows that $\text{vol}_\underline{o} \geq \frac{1}{4}\text{vol}_\bar{o}$. Combining these three inequalities gives the claim. \square

We now conclude the proof of Lemma 4.5. Suppose for contradiction that $\bar{t} - \underline{t} > \frac{192}{M} \sum_{o=\underline{o}}^{\bar{o}} n_o \cdot \text{vol}_o + 5\bar{o}$. First, since $\bar{o} \leq 2\underline{o}$, a quick calculation shows that $\text{vol}_o \geq \frac{1}{4}\text{vol}_\bar{o}$ for all o between \underline{o} and \bar{o} . Then since $|U_\ell| = \sum_{o=\underline{o}}^{\bar{o}} n_o$, our assumption implies that $\bar{t} - \underline{t} > \frac{48}{M} \cdot |U_\ell| \cdot \text{vol}_\bar{o} + 5\bar{o}$.

This further implies that w (the number of the intervals I_j of length \bar{o} in this period) is at least

$$w \geq \left\lfloor \frac{\frac{48}{M} \cdot |U_\ell| \cdot \text{vol}_\bar{o} + 5\bar{o}}{\bar{o}} \right\rfloor \geq \frac{48}{M} \cdot |U_\ell| \cdot \frac{\text{vol}_\bar{o}}{\bar{o}} + 4.$$

Every such interval I_j other than I_w has peak memory utilization more than $M - (s + \bar{o})$, otherwise the algorithm would have scheduled one more request U_ℓ in it. Then applying the previous claim to the first $\lfloor \frac{w-1}{3} \rfloor$ groups of 3 consecutive intervals I_j 's, we obtain that

$$\begin{aligned} \text{vol}_\ell(\{\underline{t}, \dots, \bar{t}\}) &\geq \left\lfloor \frac{w-1}{3} \right\rfloor \cdot \frac{1}{4} \cdot (M - (s + \bar{o})) \cdot \frac{\text{vol}_\bar{o}}{s + \bar{o}} \\ &\geq \frac{4}{M} \cdot |U_\ell| \cdot \frac{\text{vol}_\bar{o}}{\bar{o}} \cdot \frac{M}{2} \cdot \frac{\text{vol}_\bar{o}}{s + \bar{o}} > |U_\ell| \cdot \text{vol}_\bar{o}, \end{aligned} \quad (7)$$

where the second inequality uses the assumption M is twice as big as the maximum single request occupation, i.e., $s + \bar{o} \leq \frac{M}{2}$, and the last inequality uses $\text{vol}_\bar{o} = s \cdot \bar{o} + \frac{\bar{o} \cdot (\bar{o} + 1)}{2} > \frac{1}{2}\bar{o} \cdot (s + \bar{o})$.

However, each request U_ℓ contributes at most $\text{vol}_\bar{o}$ to $\text{vol}_\ell(\{\underline{t}, \dots, \bar{t}\})$, and thus $\text{vol}_\ell(\{\underline{t}, \dots, \bar{t}\}) \leq |U_\ell| \cdot \text{vol}_\bar{o}$; this contradicts Equation (7), and concludes the proof of the lemma. \square

Proof of Lemma 4.4. Let t_ℓ be the first time a request in U_ℓ is (starting to be) processed by MC-SF (let $\ell_{\max} := \lfloor \log o_{\max} \rfloor$ and let $t_{\ell_{\max}+1}$ be the last time the algorithm is processing something). The latency for each request in U_ℓ is at most $t_{\ell+1} + \bar{o}_\ell$ (i.e., if the algorithm starts processing requests from the next group then it has already started to process all requests in U_ℓ , which take at most $+\bar{o}_\ell$ time to complete); thus, the total latency is at most $\sum_\ell |U_\ell| \cdot (t_{\ell+1} + \bar{o}_\ell)$. However, from the Lemma 4.5 we know that

$$t_{\ell+1} - t_\ell \leq \frac{192}{M} \cdot |U_\ell| \cdot \text{vol}_{\bar{o}_\ell} + 5\bar{o}_\ell + 1 \leq \frac{192}{M} \cdot |U_\ell| \cdot \text{vol}_{\bar{o}_\ell} + 6\bar{o}_\ell,$$

and so $t_{\ell+1} \leq \frac{192}{M} \sum_{\ell' \leq \ell} |U_{\ell'}| \cdot \text{vol}_{\bar{o}_{\ell'}} + 6 \sum_{\ell' \leq \ell} \bar{o}_{\ell'}$.

This gives that the total latency of MC-SF can be upper bounded as

$$\text{MC-SF} \leq \frac{192}{M} \underbrace{\sum_\ell |U_\ell| \sum_{\ell' \leq \ell} |U_{\ell'}| \cdot \text{vol}_{\bar{o}_{\ell'}}}_A + 6 \underbrace{\sum_\ell |U_\ell| \sum_{\ell' \leq \ell} \bar{o}_{\ell'}}_B. \quad (8)$$

Concluding the proof of the lemma requires just a bit of algebra to clean up the bound.

To upper bound the term A , let $O_\ell := \{\underline{o}_\ell, \dots, \bar{o}_\ell\}$ be the possible output lengths of the requests in U_ℓ . We first observe that since $\bar{o}_\ell \leq 2\underline{o}_\ell$, we have $\text{vol}_{\bar{o}_\ell} \leq 4\text{vol}_{\underline{o}_\ell}$ for every $o \in O_\ell$. Moreover, since $|U_\ell| = \sum_{o \in O_\ell} n_o$, we have

$$|U_\ell|^2 \cdot \text{vol}_{\bar{o}_\ell} \leq 2 \left(\sum_{o \in O_\ell} n_o \sum_{o' \in O_\ell, o' \leq o} n_{o'} \right) \cdot \text{vol}_{\bar{o}_\ell} \leq 8 \sum_{o \in O_\ell} n_o \sum_{o' \in O_\ell, o' \leq o} n_{o'} \cdot \text{vol}_{o'}$$

and for $\ell' < \ell$

$$|U_\ell| \cdot |U_{\ell'}| \cdot \text{vol}_{\bar{o}_{\ell'}} \leq \left(\sum_{o \in O_\ell} n_o \sum_{o' \in O_{\ell'}} n_{o'} \right) \cdot \text{vol}_{\bar{o}_{\ell'}} \leq 4 \sum_{o \in O_\ell} n_o \sum_{o' \in O_{\ell'}} n_{o'} \cdot \text{vol}_{o'},$$

which combined give

$$|U_\ell| \sum_{\ell' \leq \ell} |U_{\ell'}| \cdot \text{vol}_{\bar{o}_{\ell'}} \leq 8 \sum_{o \in O_\ell} n_o \sum_{o' \leq o} n_{o'} \cdot \text{vol}_{o'},$$

and so adding up over all ℓ gives the upper bound $A \leq 8 \sum_o n_o \sum_{o' \leq o} n_{o'} \cdot \text{vol}_{o'}$.

To upper bound the term B in (8), we observe that since the \bar{o}_ℓ 's grow exponentially, $\sum_{\ell' \leq \ell} \bar{o}_{\ell'} \leq 2\bar{o}_\ell$. Then since $\bar{o}_\ell \leq 2o$ for every $o \in O_\ell$, we have

$$B \leq 2 \sum_{\ell} |U_\ell| \cdot \bar{o}_\ell = 2 \sum_{\ell} \sum_{o \in O_\ell} n_o \cdot \bar{o}_\ell \leq 4 \sum_{\ell} \sum_{o \in O_\ell} n_o \cdot o = 4 \sum_o n_o \cdot o.$$

Plugging these upper bounds on A and B on (8), we get

$$\text{MC-SF} \leq \frac{1536}{M} \sum_o n_o \sum_{o' \leq o} n_{o'} \cdot \text{vol}_{o'} + 24 \sum_o n_o \cdot o.$$

This concludes the proof of Lemma 4.4. □

Lower bound on the total latency of OPT.

Lemma 4.7. *We have the following lower bound on the total optimal latency OPT:*

$$\text{OPT} \geq \frac{1}{6M} \sum_o n_o \cdot \sum_{o' \leq o} n_{o'} \cdot \text{vol}_{o'} + \frac{1}{6} \sum_o n_o \cdot o.$$

To lower bound the total latency of OPT we consider the following LP relaxation. Let U_o denote the set of requests with output length o . Let \bar{a}_o^t be the number of requests in U_o that finish at time t in the optimal solution. The memory volume of all requests that finish up to time t need to fit in the total memory $t \cdot M$ available up to that time, and hence $\sum_{t' \leq t} \sum_o \bar{a}_o^{t'} \cdot \text{vol}_o \leq t \cdot M$. Moreover, $\sum_t \bar{a}_o^t = n_o$ (all requests in U_o finish at some time). Finally, the $\sum_o \bar{a}_o^t$ requests that finish at time t have latency (recall all requests are released at time 0) equal to t , and the optimal latency OPT is given by $\sum_t t \cdot \sum_o \bar{a}_o^t$. Together these observations show that OPT can be lower bounded by the

following Linear Program with variables a_o^t , where in particular we relax the requirement that \bar{a}_o^t 's are integers:

$$\begin{aligned}
\text{OPT}_{LP} &:= \min \sum_t t \cdot \sum_o a_o^t \\
&\text{s.t. } \sum_{t' \leq t} \sum_o a_o^{t'} \cdot \text{vol}_o \leq t \cdot M, \quad \forall t \\
&\quad \sum_t a_o^t = n_o, \quad \forall o \\
&\quad a_o^t \geq 0, \quad \forall t, o.
\end{aligned} \tag{9}$$

We then lower bound OPT_{LP} . Consider the optimal solution $\{a_o^{*t}\}_{t,o}$ for this LP. For a given output size o , let t_o^* be the first time t where $a_o^{*t} > 0$, i.e., where a request U_o is assigned to time t .

Indeed we can see the above LP as the problem of, for each o , (fractionally) assigning n_o units over the time steps $0, 1, \dots$ subject to the constraint that the time steps have a limited receiving capacity, and assigning a unit to time t incurs a cost of t . Since vol_o is increasing over o , we observe that that optimal solution to this LP is to first try to assign all requests with the smallest o (call it o_{\min}) to time 1; if the constraint $\sum_o a_o^1 \cdot \text{vol}_o \leq M$ does not allow all $n_{o_{\min}}$ requests to be assigned to time 1, the remaining ones are assigned to time 2, and so on; otherwise we move to the *2nd* smallest o and assign the requests U_o to time 1. This optimizes the above LP because it maximizes the number of items assigned to time 1, which has the smallest cost (the analogous argument holds for the other times). In summary, we have that the ‘‘first time’’ values t_o^* are non-decreasing, namely $t_o^* \leq t_{o'}^*$ when $o < o'$.

Let $t_{o_{\max}+1}^*$ be the last time such that $\sum_o a_o^{*t} > 0$. Using this observation we will prove the following lower bound on the ‘‘first times’’ t_o^* .

Claim 4.8. For all o we have $t_{o+1}^* \geq \frac{1}{M} \sum_{o' \leq o} n_{o'} \cdot \text{vol}_{o'}$.

Proof. By the observation above, in the optimal solution $\{a_o^{*t}\}_{o,t}$ all items with output length at most o are assigned to times $\leq t_{o+1}^*$, i.e., no later than when the next output length is assigned; thus, $\sum_{t' \leq t_{o+1}^*} a_{o'}^{*t'} = n_{o'}$ for all $o' \leq o$. Then considering (9) to time t_{o+1}^* we get

$$\sum_{o' \leq o} n_{o'} \cdot \text{vol}_{o'} = \sum_{t' \leq t_{o+1}^*} \sum_{o' \leq o} a_{o'}^{*t'} \cdot \text{vol}_{o'} \leq t_{o+1}^* \cdot M,$$

and rearranging we get the claim. □

We are now able to prove the lower bound on OPT from Lemma 4.7.

Proof of Lemma 4.7. By definition of t_o^* , we know that $a_o^{*t} = 0$ for all $t < t_o^*$, and so $\sum_t t \cdot a_o^{*t} \geq t_o^* \cdot \sum_{t \geq t_o^*} a_o^{*t} = t_o^* \cdot n_o$. Plugging the bound on t_o^* from the previous claim and adding over all o we

can lower bound OPT_{LP} (and thus OPT) as

$$\begin{aligned}
\text{OPT} &\geq \text{OPT}_{LP} = \sum_t t \cdot \sum_o a_o^{*t} \\
&\geq \sum_o n_o \cdot t_o^* \\
&\geq \sum_o n_o \cdot \left(\frac{1}{M} \sum_{o' < o} n_{o'} \cdot \text{vol}_{o'} \right) \\
&= \frac{1}{M} \sum_o n_o \sum_{o' \leq o} n_{o'} \cdot \text{vol}_{o'} - \frac{1}{M} \sum_o n_o^2 \cdot \text{vol}_o. \tag{10}
\end{aligned}$$

To remove the negative term in the right-hand side (and add a new one, to match that of Lemma 4.4), we provide two other lower bounds on the original OPT (not the LP).

The first is that for any output length o , due to memory constraints, at most $\frac{n_o}{2}$ of them can be finished in the optimal schedule by time $\frac{n_o}{2} \frac{\text{vol}_o}{M}$, since the total memory available up to this time is $\frac{n_o}{2} \cdot \text{vol}_o$ and each such request consumes vol_o memory; thus, the total latency on the optimal solution for the request of output length o is at least $\frac{n_o}{2} \cdot \frac{n_o}{2} \frac{\text{vol}_o}{M}$. Adding this over all o , the total latency OPT has the lower bound

$$\text{OPT} \geq \frac{1}{4M} \sum_o n_o^2 \cdot \text{vol}_o. \tag{11}$$

Finally, since each request of output length o takes $(o + 1)$ units of processing/time to finish (and thus has latency at least o), we also have $\text{OPT} \geq \sum_o n_o \cdot o$ (which is at least $\sum_o n_o$).

Adding this bound plus 4 times (11) plus (10) we get

$$6 \text{OPT} \geq \frac{1}{M} \sum_o n_o \sum_{o' \leq o} n_{o'} \cdot \text{vol}_{o'} + \sum_o n_o \cdot o. \tag{12}$$

This concludes the proof of Lemma 4.7. □

Combining the bound on MC-SF from Lemma 4.4 and the lower bound on OPT from Lemma 4.7, we obtain $\text{MC-SF} \leq O(1) \cdot \text{OPT}$, thus proving the first part of the theorem. The proof for the second part of the theorem can be found in Appendix B. □

5 Numerical Simulation

In this section, we conduct numerical simulations using both synthetic data and real-world traces to evaluate the performance of our proposed scheduling algorithm MC-SF .

In the first of these experiments (Section 5.1), the primary goal of is to assess the performance of MC-SF within the framework of the mathematical model introduced in Sections 2, comparing it against the hindsight-optimal policy from Section 3. The second set of experiment (Section 5.2) evaluates the practical effectiveness of MC-SF using a large-scale, open-source dataset derived from real LLM inference traces. Due to the size and complexity of this dataset, it is computationally

infeasible to compute the hindsight optimal-solution, and we instead compare MC-SF against several baseline scheduling policies that are representative of those used in real-world LLM inference systems. Additional experimental results are provided in Appendix C.

5.1 Synthetic Data Numerical Simulations

We first evaluate the performance of MC-SF on synthetic datasets. These experiments aim to quantify the two primary sources of performance gap between the algorithm and the hindsight optimal: (i) the information asymmetry between online and offline algorithms, and (ii) the inherent suboptimality of the algorithm itself. To partially disentangle these effects, we consider two different arrival models.

To obtain the hindsight-optimal solution, we solve the integer programming model from Section 3 using the Gurobi solver. Since solving the Integer Program is computationally expensive, we limit this comparison to small-scale synthetic instances to meet reasonable memory and time limits.

Experimental Setup. For each experiment, the memory capacity M is drawn uniformly from the integers between 30 and 50. For each request, the prompt size s_i is drawn uniformly from the integers between 1 and 5, and the output length o_i from the integers between 1 and $M - s_i$. We run 200 independent trials under each of the following arrival models:

1. *Arrival Model 1 (All-at-once arrivals).* All n requests arrive at time $t = 0$, where n is a random integer between 40 and 60. This model allows both MC-SF and the hindsight optimal to access the full set of requests at the beginning of execution, eliminating any information gap. Therefore, any observed performance difference is solely due to the algorithm’s structural approximation.
2. *Arrival Model 2 (Online stochastic arrivals).* Requests arrive over a discrete time horizon $[1, T]$, where T is drawn uniformly from the integers between 40 and 60. The arrival process follows a stationary Poisson distribution with rate λ , where $\lambda \in [0.5, 1.5]$ is sampled uniformly. This now introduces online uncertainty, which the algorithm must respond to without knowing future arrivals.

Performance Metric. We evaluate performance using the ratio between the total end-to-end latency incurred by MC-SF and that of the hindsight-optimal policy. A ratio of 1 indicates that the algorithm achieves the optimal schedule, while larger values reflect a performance gap.

Results for Arrival Model 1. Across 200 trials, the best-case ratio is 1.000 (meaning the algorithm produces the optimal schedule), the worst-case ratio is 1.074, while the average ratio is 1.005. The left figure of Figure 2 displays the distribution of latency ratio of MC-SF vs. Hindsight Optimal under Arrival Model 1. These results show that in this setting, MC-SF performs almost optimally. In 114 of the 200 trials, the algorithm exactly matches the optimal latency, demonstrating that its design closely approximates the structure of the hindsight-optimal policy. Since in this first arrival model there is no information gap between MC-SF and hindsight-optimum, both having full knowledge of the input, these ratios close to 1 indicate that our proposed algorithm has a very small structural suboptimality.

Results for Arrival Model 2. Across 200 trials, here the best-case ratio is 1.000, the worst-case ratio is 1.227, and the average ratio is 1.047. The right figure of Figure 2 displays the distribution of latency ratio of MC-SF vs. Hindsight Optimal under Arrival Model 2. Since now the items are

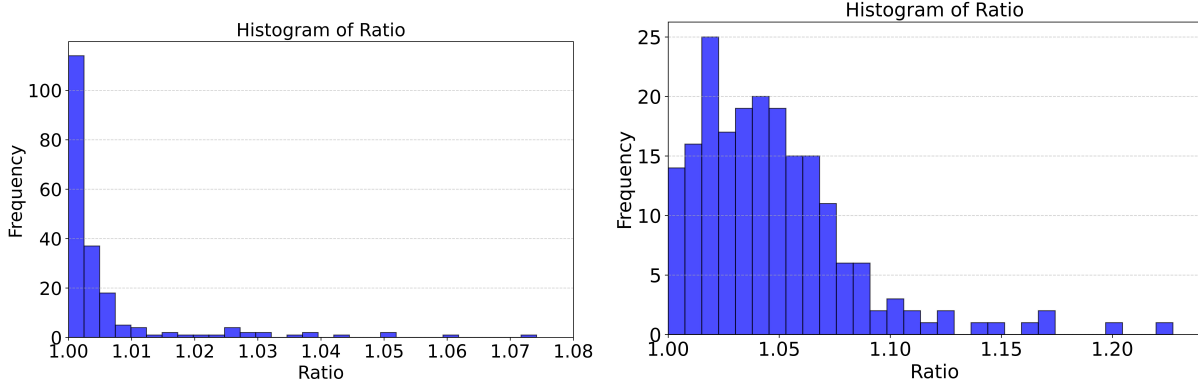


Figure 2: Histogram of latency ratio: MC-SF vs. Hindsight Optimal. **Left:** Arrival Model 1. **Right:** Arrival Model 2.

not known a priori by the algorithm, the performance ratio captures both the effect of information asymmetry and the algorithm’s structural approximation error. The resulting ratios are still quite close to 1, indicating strong performance of MC-SF and establishing it as an effective and practically viable scheduling policy. The difference of the ratios between the two models can be partially attributed to the cost of online decision-making.

5.2 Real Data Numerical Experiments

Dataset Overview. We use a conversational dataset³ by Zheng et al. [2023] from over 210,000 distinct IP addresses via the Vicuna demo and Chatbot Arena platforms. To manage its size, we selected a random subset of 10,000 conversations for analysis. Each conversation includes a user-generated question and a response from an LLM. We define the question as the prompt input and each word in the response as an output token. Figure 5 in Appendix C shows the distribution of the sizes (word count) of prompts (mean: 40.62 and median: 11) and output tokens (mean: 85.32 and median: 45).

Simulation Setup. In our simulation, we operate over a continuous time horizon, with 10,000 prompts arriving according to a stationary Poisson process. Let λ denote the arrival rate per second, where we consider two cases: **Case 1: High Demand** $\lambda = 50$ and **Case 2: Low Demand** $\lambda = 10$. In both scenarios, we simulate the performance of the Llama2-70B model on two linked A100 GPUs (operating collectively as a single worker) and consider the memory limit $M = 16492$; additional details can be found in Appendix C.

At a high level, our simulation works as follows: prompts chosen from the conversational dataset arrive continuously according to the chosen Poisson arrival process. To calculate the processing time of a batch created by an algorithm, we use LLM inference simulator from Agrawal et al. [2024a].⁴ We then report average end-to-end latency, i.e., the total end-to-end latency divided by the number of requests.

³Publicly available at <https://huggingface.co/datasets/lmsys/lmsys-chat-1m>.

⁴Publicly available at <https://github.com/microsoft/vidur/>.

Benchmark Algorithms. Currently, most LLM inference research is built on vLLM, a widely recognized high-performance inference engine designed to enhance the efficiency of Large Language Model (LLM) inference [Kwon et al., 2023]. Since LLM inference is a relatively new field, scheduling algorithms in both academia and industry primarily rely on those implemented in vLLM. The scheduling algorithm in vLLM follows a first-come, first-served (FCFS) strategy: when the machine is idle, it prioritizes requests based on their arrival time. However, instead of maximizing the number of requests in a batch, vLLM uses a predefined threshold for memory occupation. Once the KV cache occupancy exceeds this threshold, no additional requests are added to the batch. This motivates us to define the following benchmarks:

α -protection greedy algorithms. We begin with a class of parameterized algorithms called α -protection greedy scheduling algorithms, where $\alpha \in (0, 1)$. These algorithms maintain a protection memory threshold of αM , serving as a safeguard against memory overflow. When forming each batch, the algorithm gives priority to existing token jobs. For new prompt requests, it checks if adding a new prompt i with initial memory $s_i + 1$ would cause the memory usage to exceed $(1 - \alpha)M$. If the memory limit is exceeded, no further prompts are added to the batch. In the event that the KV cache memory overflows during the processing of the requests, the α -protection greedy scheduling algorithms will clear all active requests sending them back to the waiting queue as unprocessed.

α -protection, β -clearing algorithms. α -protection greedy scheduling algorithms can cause unnecessary evictions; to address this, we define a new class of benchmark algorithms: α -protection β -clearing algorithms. These algorithms follow the same principles as α -protection greedy scheduling but, when the KV cache memory limit is exceeded, each active request is cleared and sent back to the scheduler with an independent probability β .

Memory Constrained Benchmark (MC-Benchmark). Beyond the benchmarks discussed above, we introduce an additional benchmark algorithm, denoted as MC-Benchmark, which is partially inspired by the vLLM scheduling policy and partially by the memory feasibility checks used in MC-SF. Following the vLLM structure, MC-Benchmark forms batches by processing requests in ascending order of their arrival times. While constructing a batch, it decides whether to include each request based on a prospective memory check used in MC-SF: it only adds a request if the future memory usage, including KV cache growth, remains within the memory limit M . The detailed pseudocode for MC-Benchmark is provided in Appendix C (Algorithm 2).

5.2.1 Results: High vs. Low Demand

We evaluate the performance of MC-SF and baseline algorithms under two demand regimes: high demand ($\lambda = 50$) and low demand ($\lambda = 10$).

First, we examine memory usage over time. Figures 6 and 9 show that MC-SF consistently stays within the memory limit M across both settings. Despite batch processing durations varying in practice, the memory check in Equation (6) reliably prevents overflow by ensuring feasibility over future memory usage. Under low demand, memory usage remains close to full utilization, suggesting a stable system state.

We also investigate the performance of the α -protection and α -protection- β -clearing heuristics. We observe that for very small protection levels α , the α -protection heuristic may lead to repeated

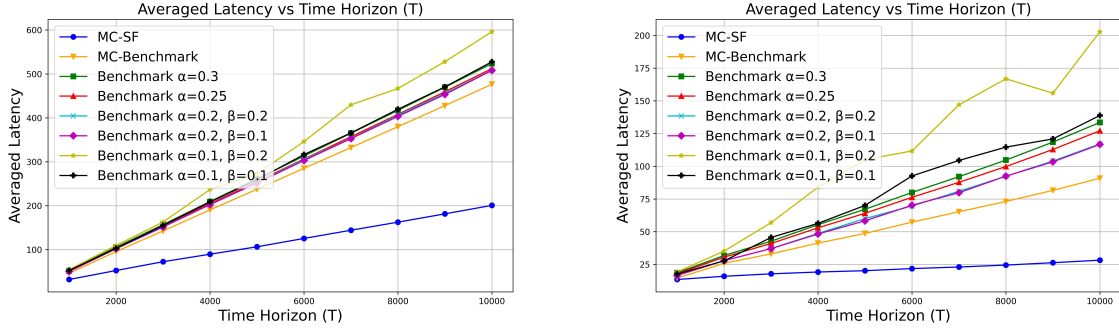


Figure 3: Average End-to-End Latency Across Scheduling Algorithms. **Left:** High Demand. **Right:** Low Demand.

evictions and infinite processing loops, therefore we perform a grid search with step size 0.01 to identify the smallest possible α : $\alpha = 0.21$ in the high-demand setting and $\alpha = 0.24$ in the low-demand setting. We then evaluate latency across six configurations, including $\alpha = 0.3$, $\alpha = 0.25$, and four combinations of $\alpha \in \{0.2, 0.1\}$, $\beta \in \{0.2, 0.1\}$.

Figure 3 presents the average end-to-end latency across all algorithms for request volumes $\{1000, 2000, \dots, 10000\}$. In the high-demand case (left), average latency increases linearly for all algorithms, indicating overload. Notably, MC-SF has a slope of approximately $1/6$, compared to $1/2$ for the best-performing benchmark, highlighting its superior scalability. In the low-demand case (right), MC-SF maintains a much lower latency growth rate—about $1/800$, which is over eight times smaller than the best benchmark slope ($\sim 1/100$).

These results confirm that MC-SF remains memory-safe and highly efficient across both regimes. Additional results are also provided in Appendix C.

6 Discussion

In this work, we studied a model for scheduling in LLM inference. There are several research directions that stem from our work.

Our model in Section 2 relies on the assumption that the decision-maker can perfectly predict the output length of each prompt request upon arrival. However, as we noted in Section 2, while practical methods exist for predicting output length, they are subject to errors. One of the most important next steps in the optimization for LLM inference agenda is to go beyond perfect prediction for the request output length. Note that inaccurate predictions—unless accounted for by a specific algorithm—may lead to memory usage that exceeds the KV cache size thus causing the computational worker to stop until the memory is cleared.

Our algorithm can already provide a starting point for this new model. To see this, assume that there exists a bound δ (known to the decision-maker) such that, with high probability, the true output length o_i and its predicted value \hat{o}_i satisfy $|o_i - \hat{o}_i| \leq \delta, \forall i$. Upon a prompt’s arrival, the decision-maker has access to \hat{o}_i but not o_i . One way to ensure that an online scheduling algorithm avoids memory overflow is to replace all o_i with $\hat{o}_i + \delta$, the upper bound on output length. However,

this approach is overly conservative and can be highly inefficient if δ is large. To effectively address robust scheduling in the presence of inaccurate prompt output predictions, the model must also incorporate a mechanism for managing and clearing KV cache overflows.

Another research avenue of great potential is to study the case where there are multiple computational workers that can work in parallel. Finally, we think that it would be interesting to study a scheduling setting where most of the requests follow a stochastic pattern from some unknown distribution, but there is a small number of requests that are extraordinarily big or small.

Acknowledgements

The authors are grateful to Esha Choukse, Íñigo Goiri, Rodrigo Fonseca, and Chaojie Zhang from Azure Research Systems, and Ishai Menache, Sebastian Burckhardt, and Aashaka Shah from Microsoft Research for helpful discussions. PJ acknowledges funding from AFOSR grant FA9550-23-1-0190 and ONR grant N00014-24-1-2470. CP was supported by an Amazon Research Award. JJ was supported by the Early Career Scheme (ECS) 26210223 from Research Grants Council, Hong Kong.

References

- Amey Agrawal, Ashish Panwar, Jayashree Mohan, Nipun Kwatra, Bhargav S Gulavani, and Ramachandran Ramjee. Sarathi: Efficient LLM inference by piggybacking decodes with chunked prefills. *arXiv preprint arXiv:2308.16369*, 2023.
- Amey Agrawal, Nitin Kedia, Jayashree Mohan, Ashish Panwar, Nipun Kwatra, Bhargav Gulavani, Ramachandran Ramjee, and Alexey Tumanov. Vidur: A large-scale simulation framework for LLM inference. *Proceedings of Machine Learning and Systems*, 6:351–366, 2024a.
- Amey Agrawal, Nitin Kedia, Ashish Panwar, Jayashree Mohan, Nipun Kwatra, Bhargav S Gulavani, Alexey Tumanov, and Ramachandran Ramjee. Taming throughput-latency tradeoff in LLM inference with Sarathi-Serve. *arXiv preprint arXiv:2403.02310*, 2024b.
- Kunal Agrawal, Jing Li, Kefu Lu, and Benjamin Moseley. Scheduling parallel dag jobs online to minimize average flow time. In *Proceedings of the Twenty-Seventh Annual ACM-SIAM Symposium on Discrete Algorithms*, SODA '16, page 176–189, USA, 2016. Society for Industrial and Applied Mathematics. ISBN 9781611974331.
- Susanne Albers. Online algorithms: a survey. *Math. Program.*, 97(1-2):3–26, 2003. doi: 10.1007/S10107-003-0436-0. URL <https://doi.org/10.1007/s10107-003-0436-0>.
- Susanne Albers. Online scheduling. In *Introduction to scheduling*, pages 71–98. CRC Press, 2009.
- Amazon. Amazon CodeWhisperer. <https://aws.amazon.com/codewhisperer/>, 2023.
- Anthropic. Claude. <https://claude.ai>, 2023.
- Yossi Azar and Leah Epstein. On-line scheduling with precedence constraints. *Discrete Applied Mathematics*, 119(1):169–180, 2002. ISSN 0166-218X. doi: [https://doi.org/10.1016/S0166-218X\(01\)00272-4](https://doi.org/10.1016/S0166-218X(01)00272-4). URL <https://www.sciencedirect.com/science/article/>

- [pii/S0166218X01002724](https://doi.org/10.1007/978-3-031-18007-2_1). Special Issue devoted to Foundation of Heuristics in Combinatorial Optimization.
- Tom Brown, Benjamin Mann, Nick Ryder, Melanie Subbiah, Jared D Kaplan, Prafulla Dhariwal, Arvind Neelakantan, Pranav Shyam, Girish Sastry, Amanda Askell, et al. Language models are few-shot learners. *Advances in neural information processing systems*, 33:1877–1901, 2020.
- Marco Cascella, Jonathan Montomoli, Valentina Bellini, and Elena Bignami. Evaluating the feasibility of ChatGPT in healthcare: an analysis of multiple clinical and research scenarios. *Journal of medical systems*, 47(1):33, 2023.
- Character. Character ai. <https://character.ai>, 2021.
- Aakanksha Chowdhery, Sharan Narang, Jacob Devlin, Maarten Bosma, Gaurav Mishra, Adam Roberts, Paul Barham, Hyung Won Chung, Charles Sutton, Sebastian Gehrmann, et al. Palm: Scaling language modeling with pathways. *Journal of Machine Learning Research*, 24(240):1–113, 2023.
- Naveen Garg, Anupam Gupta, Amit Kumar, and Sahil Singla. Non-clairvoyant precedence constrained scheduling. In Christel Baier, Ioannis Chatzigiannakis, Paola Flocchini, and Stefano Leonardi, editors, *46th International Colloquium on Automata, Languages, and Programming, ICALP 2019, July 9-12, 2019, Patras, Greece*, volume 132 of *LIPICs*, pages 63:1–63:14. Schloss Dagstuhl - Leibniz-Zentrum für Informatik, 2019. doi: 10.4230/LIPICs.ICALP.2019.63. URL <https://doi.org/10.4230/LIPICs.ICALP.2019.63>.
- GilPress. ChatGPT users statistics. WhatsTheBigData, 2024. URL https://whatsthebigdata.com/chatgpt-users/#google_vignette.
- GitHub. GitHub copilot. <https://github.com/features/copilot>, 2021.
- Google. Bard. <https://bard.google.com>, 2023.
- Cindy Gordon. ChatGPT and Generative AI innovations are creating sustainability havoc. Forbes, 2024. URL <https://www.forbes.com/sites/cindygordon/2024/03/12/chatgpt-and-generative-ai-innovations-are-creating-sustainability-havoc/>.
- Öncü Hazır and Safia Kedad-Sidhoum. Batch sizing and just-in-time scheduling with common due date. *Annals of Operations Research*, 213:187–202, 2014.
- Coleman Hooper, Sehoon Kim, Hiva Mohammadzadeh, Michael W Mahoney, Yakun Sophia Shao, Kurt Keutzer, and Amir Gholami. Kvquant: Towards 10 million context length LLM inference with KV cache quantization. *arXiv preprint arXiv:2401.18079*, 2024.
- Sungjin Im and Benjamin Moseley. Online batch scheduling for flow objectives. In *Proceedings of the twenty-fifth annual ACM symposium on Parallelism in algorithms and architectures*, pages 102–104, 2013.
- Hao Kang, Qingru Zhang, Souvik Kundu, Geonhwa Jeong, Zaoxing Liu, Tushar Krishna, and Tuo Zhao. Gear: An efficient KV cache compression recipe for near-lossless generative inference of LLM. *arXiv preprint arXiv:2403.05527*, 2024.

- Jared Kaplan, Sam McCandlish, Tom Henighan, Tom B Brown, Benjamin Chess, Rewon Child, Scott Gray, Alec Radford, Jeffrey Wu, and Dario Amodei. Scaling laws for neural language models. *arXiv preprint arXiv:2001.08361*, 2020.
- Ali Husseinzadeh Kashan and Behrooz Karimi. Scheduling a single batch-processing machine with arbitrary job sizes and incompatible job families: an ant colony framework. *Journal of the Operational Research Society*, 59(9):1269–1280, 2008.
- Komo. Komo AI. <https://komo.ai/>, 2023.
- Woosuk Kwon, Zhuohan Li, Siyuan Zhuang, Ying Sheng, Lianmin Zheng, Cody Hao Yu, Joseph Gonzalez, Hao Zhang, and Ion Stoica. Efficient memory management for large language model serving with PagedAttention. In *Proceedings of the 29th Symposium on Operating Systems Principles*, pages 611–626, 2023.
- Joseph Y.-T. Leung, editor. *Handbook of Scheduling - Algorithms, Models, and Performance Analysis*. Chapman and Hall/CRC, 2004. ISBN 978-1-58488-397-5. URL <http://www.crcnetbase.com/isbn/978-1-58488-397-5>.
- Wenhua Li, Libo Wang, Xing Chai, and Hang Yuan. Online batch scheduling of simple linear deteriorating jobs with incompatible families. *Mathematics*, 8(2):170, 2020.
- Pierre Lienhart. LLM inference series: 2. The two-phase process behind LLMs’ responses. <https://medium.com/@plienhar/>, 2023.
- Aixin Liu, Bei Feng, Bin Wang, Bingxuan Wang, Bo Liu, Chenggang Zhao, Chengqi Deng, Chong Ruan, Damai Dai, Daya Guo, et al. Deepseek-v2: A strong, economical, and efficient mixture-of-experts language model. *arXiv preprint arXiv:2405.04434*, 2024.
- Peihai Liu and Xiwen Lu. Online unbounded batch scheduling on parallel machines with delivery times. *Journal of Combinatorial Optimization*, 29:228–236, 2015.
- Brendan Lucier, Ishai Menache, Joseph Naor, and Jonathan Yaniv. Efficient online scheduling for deadline-sensitive jobs. In *Proceedings of the twenty-fifth annual ACM symposium on Parallelism in algorithms and architectures*, pages 305–314, 2013.
- Microsoft. Bing AI. <https://www.bing.com/chat>, 2023.
- OpenAI. ChatGPT. <https://chat.openai.com>, 2019.
- OpenAI. GPT-4 technical report. arxiv 2303.08774. *View in Article*, 2(5), 2023.
- Pratyush Patel, Esha Choukse, Chaojie Zhang, Aashaka Shah, Íñigo Goiri, Saeed Maleki, and Ricardo Bianchini. Splitwise: Efficient generative LLM inference using phase splitting. *Power*, 400(700W):1–75, 2023.
- Cheng Peng, Xi Yang, Aokun Chen, Kaleb E Smith, Nima PourNejatian, Anthony B Costa, Cheryl Martin, Mona G Flores, Ying Zhang, Tanja Magoc, et al. A study of generative large language model for medical research and healthcare. *NPJ digital medicine*, 6(1):210, 2023.
- Perplexity. Perplexity AI. <https://www.perplexity.ai/>, 2022.
- Michael L Pinedo. *Scheduling*, volume 29. Springer, 2012.

- Reiner Pope, Sholto Douglas, Aakanksha Chowdhery, Jacob Devlin, James Bradbury, Jonathan Heek, Kefan Xiao, Shivani Agrawal, and Jeff Dean. Efficiently scaling transformer inference. *Proceedings of Machine Learning and Systems*, 5:606–624, 2023.
- Chris N Potts and Mikhail Y Kovalyov. Scheduling with batching: A review. *European journal of operational research*, 120(2):228–249, 2000.
- Replit. Replit ghostwriter. <https://replit.com/site/ghostwriter>, 2018.
- Julien Robert and Nicolas Schabanel. Non-clairvoyant scheduling with precedence constraints. In Shang-Hua Teng, editor, *Proceedings of the Nineteenth Annual ACM-SIAM Symposium on Discrete Algorithms, SODA 2008, San Francisco, California, USA, January 20-22, 2008*, pages 491–500. SIAM, 2008. URL <http://dl.acm.org/citation.cfm?id=1347082.1347136>.
- Tim Roughgarden, editor. *Beyond the Worst-Case Analysis of Algorithms*. Cambridge University Press, 2020. ISBN 9781108637435. doi: 10.1017/9781108637435. URL <https://doi.org/10.1017/9781108637435>.
- Malik Sallam. The utility of ChatGPT as an example of large language models in healthcare education, research and practice: Systematic review on the future perspectives and potential limitations. *MedRxiv*, pages 2023–02, 2023.
- Ying Sheng, Lianmin Zheng, Binhang Yuan, Zhuohan Li, Max Ryabinin, Beidi Chen, Percy Liang, Christopher Ré, Ion Stoica, and Ce Zhang. Flexgen: High-throughput generative inference of large language models with a single GPU. In *International Conference on Machine Learning*, pages 31094–31116. PMLR, 2023.
- Yan Sun. The economics of large language models. Substack, 2023. URL <https://sunyan.substack.com/p/the-economics-of-large-language-models>.
- Ashish Vaswani, Noam Shazeer, Niki Parmar, Jakob Uszkoreit, Llion Jones, Aidan N Gomez, Lukasz Kaiser, and Illia Polosukhin. Attention is all you need. *Advances in neural information processing systems*, 30, 2017.
- Jason Wei, Yi Tay, Rishi Bommasani, Colin Raffel, Barret Zoph, Sebastian Borgeaud, Dani Yogatama, Maarten Bosma, Denny Zhou, Donald Metzler, et al. Emergent abilities of large language models. *arXiv preprint arXiv:2206.07682*, 2022.
- Fan Yang, Morteza Davari, Wenchao Wei, Ben Hermans, and Roel Leus. Scheduling a single parallel-batching machine with non-identical job sizes and incompatible job families. *European Journal of Operational Research*, 303(2):602–615, 2022.
- You.com. You.com. <https://you.com/>, 2020.
- Gyeong-In Yu, Joo Seong Jeong, Geon-Woo Kim, Soojeong Kim, and Byung-Gon Chun. Orca: A distributed serving system for {Transformer-Based} generative models. In *16th USENIX Symposium on Operating Systems Design and Implementation (OSDI 22)*, pages 521–538, 2022.
- Lianmin Zheng, Wei-Lin Chiang, Ying Sheng, Tianle Li, Siyuan Zhuang, Zhanghao Wu, Yonghao Zhuang, Zhuohan Li, Zi Lin, Eric Xing, et al. LMSYS-Chat-1M: A large-scale real-world LLM conversation dataset. *arXiv preprint arXiv:2309.11998*, 2023.

- Zangwei Zheng, Xiaozhe Ren, Fuzhao Xue, Yang Luo, Xin Jiang, and Yang You. Response length perception and sequence scheduling: An LLM-empowered LLM inference pipeline. *Advances in Neural Information Processing Systems*, 36, 2024.
- Yinmin Zhong, Shengyu Liu, Junda Chen, Jianbo Hu, Yibo Zhu, Xuanzhe Liu, Xin Jin, and Hao Zhang. Distserve: Disaggregating prefill and decoding for goodput-optimized large language model serving. *arXiv preprint arXiv:2401.09670*, 2024.
- Banghua Zhu, Ying Sheng, Lianmin Zheng, Clark Barrett, Michael I Jordan, and Jiantao Jiao. On optimal caching and model multiplexing for large model inference. In *Proceedings of the 37th International Conference on Neural Information Processing Systems*, pages 59062–59094, 2023.

Supplementary Material for paper *“Online Scheduling for LLM Inference with KV Cache Constraints”*

A Background: Online Optimization in LLM Inference

This section provides background in LLM inference using a single computational worker (i.e., a single GPU).

A.1 LLM Inference Process on a Single Request

We first demonstrate how a single GPU worker processes an incoming prompt, using the example prompt “What color is the sky?” from Lienhart [2023]. The workflow is illustrated in Figure 4.

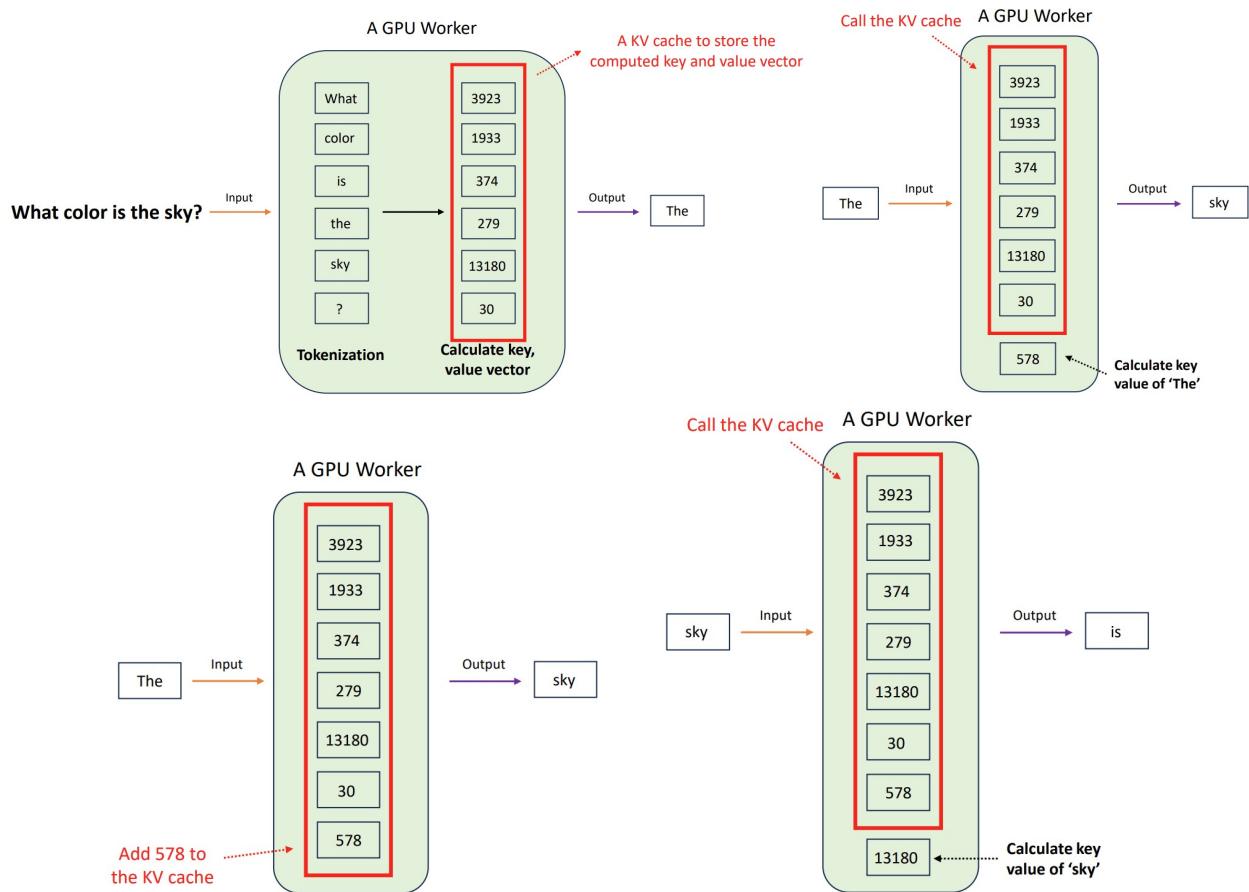


Figure 4: An example of LLM inference [Lienhart, 2023].

Upon receiving the prompt, as shown in the top left figure, the worker begins by tokenizing the prompt and generates key and value vectors. Then, it uses these vectors to calculate the attention

scores, which indicate the relevance of each token, enabling the generation of the first output token, “The.” To avoid recalculating these vectors with each new token, the worker saves them in a key-value (KV) cache.

Next, as depicted in the top right figure, after generating “The,” the worker processes this token by calculating its key and value and retrieving the key-value vectors of the initial prompt tokens from the KV cache. Using this combined data, the model generates the next token, “sky.”

The bottom left figure shows that during “sky” generation, the worker calculates the key and value for “The” and adds them to the KV cache to avoid recalculations. Finally, as illustrated in the bottom right figure, the worker processes “sky,” continuing this cycle until all output tokens are generated.

Finally, we note that when a prompt request arrives, the computational worker does not know the length of its response (i.e., the number of tokens it will generate). However, certain techniques can predict the output length of each prompt before processing begins. For instance, [Zheng et al. \[2024\]](#) proposes a methodology that achieves an output length prediction accuracy of up to 81%.

A.2 Illustration of Novel Difficult Aspects of LLM Inference Scheduling

Though scheduling problems have been studied extensively in the previous literature on computing resource allocation (e.g., [Pinedo \[2012\]](#)), we illustrate some of the new dynamics of LLM inference that separates it from standard scheduling problems. To be specific, due to the autoregressive LLM inference process described in [A.1](#), the memory size required by a request keeps growing during the inference procedure, which is fundamentally different from the previous scheduling models where the size (or the resource occupation) of a job is fixed.

To see this point, suppose that we are following the principle of processing the shortest job first and there are two prompts P1 and P2, whose sizes eventually grow to t_1 and t_2 . If $t_1 + t_2 > M$, where M is the memory limit of the KV cache, then the two prompts cannot be processed at the same time in the classical scheduling model. However, this may not be the case for our LLM inference model since the sizes are varying over time. Suppose that the initial size for both prompts is the same, denoted by s , and it satisfies that $s \leq t_1 \leq M/2$. The size of both jobs increases by 1 at each round until reaching t_1 and t_2 . Then, we can process P1 and P2 at the same time until the time $t_1 - s$ where the size of both jobs increases to t_1 , since the memory requirement for the two jobs is upper bounded $2t_1 \leq M$. After time $t_1 - s$, though the size of P2 may be larger than t_1 , the prompt P1 has finished processing, and the required memory can be released to further process P2. Therefore, P1 and P2 can be processed at the same time in the LLM inference model.

Moreover, the batching problem in our setting significantly differs from traditional problems (e.g., [Potts and Kovalyov \[2000\]](#)). When assuming that the KV cache memory limit is the sole constraint for the batch size, the number of jobs in a batch during each round varies depending on the specific jobs included in the batch. This is because the memory usage for each output token increases linearly over time. While some studies ([Kashan and Karimi \[2008\]](#), [Hazır and Kedad-Sidhoum \[2014\]](#), [Yang et al. \[2022\]](#)) consider batch size constraints as the total weight of jobs—where weight corresponds to the memory usage of each prompt or token—in our problem, the situation is more complex. Processing a prompt or token increases the memory usage. Consequently, the effective weight of jobs at any given time depends on the starting time to process this token, and the index

of this token in the request. This weight dependency also makes the problem more challenging.

B Appendix for Section 4

B.1 Proof of Theorem 4.1

Proof of Theorem 4.1. Fix a deterministic algorithm \mathcal{A} . For any $M \geq 1$, consider the following instance \mathcal{I} with available memory M and with $s_i = 1$ for all request i . First, a request is released at time 0 with output length $o_1 = M - 1$ (“long request”). Let b be the time \mathcal{A} starts processing this first request. Then $\frac{M}{2}$ requests are released at time $r := b + M - \frac{\sqrt{M}}{2}$ with output size $o_i = 1$ (“short requests”). Let $n := \frac{M}{2} + 1$ denote the number of requests in this instance. We claim that the total latency of \mathcal{A} on this instance is at least $\Omega(\sqrt{n}) \cdot \text{OPT}(\mathcal{I})$.

For that, we first claim that

$$\text{OPT}(\mathcal{I}) \leq 3.5M. \quad (13)$$

If $r \geq M$, then it is possible to start processing the long request at time 0 and finish by time $M - 1$ (incurring latency $M - 1$) and then at time $r \geq M$ start processing all the short requests (since the maximum memory occupation of each short request is 2, they can all be executed together), finishing them at time $r + 1$ (incurring latency 1 for each of these requests); in this case we have $\text{OPT}(\mathcal{I}) \leq M - 1 + \frac{M}{2} \leq 3.5M$ as desired.

If $r < M$, then a possible offline solution is to first do all the short requests and then the long request, namely start executing all the short requests at time r , finishing them at time $r + 1$ (incurring latency 1 for each), and then start to process the long request at time $r + 2$, finishing it at time $r + 2 + (M - 1)$ (incurring latency $r + 2 + (M - 1)$). Therefore, $\text{OPT}(\mathcal{I}) \leq \frac{M}{2} + r + 1 + M \leq 2.5M + 1 \leq 3.5M$, where the second inequality uses the fact we are in the case $r < M$ and the last inequality uses $M \geq 1$. Thus, in both cases we have that (13) holds.

We now lower bound the latency that \mathcal{A} experiences over \mathcal{I} . In all times between time $r = b + (M - 1) - \frac{\sqrt{M}}{2}$ and $b + (M - 1)$, the long request occupies memory at least $M - \frac{\sqrt{M}}{2}$; thus, the total memory available for other requests across all those times is at most $\frac{\sqrt{M}}{2} \cdot \frac{\sqrt{M}}{2} = \frac{M}{4}$. Thus, at least $\frac{M}{2} - \frac{M}{4} = \frac{M}{4}$ of the short requests can only be started by the algorithm \mathcal{A} on or after time $b + M$, and thus each of them incurs latency at least $b + M - r = \frac{\sqrt{M}}{2}$. Thus, the total latency of \mathcal{A} is at least $\frac{M}{4} \cdot \frac{\sqrt{M}}{2}$.

Combining this with the upper bound on OPT from (13), we get

$$\frac{\text{TEL}(\mathcal{I}; \mathcal{A})}{\text{OPT}(\mathcal{I})} \geq \frac{\sqrt{M}}{28}.$$

Since the number of items in the instance is $n = 1 + \frac{M}{2}$, this shows that the competitive ratio of \mathcal{A} cannot be better than $\Omega(\sqrt{n})$, thus proving the theorem. \square

B.2 Proof of Proposition 4.2

Proof of Proposition 4.2. At each time step $t \in [T]$, to solve Eq. (6), we add requests in ascending order of their indices, stopping the process once any inequality is violated. The memory limit M is

a constant, which implies that we will add at most $M/(\max_{i \in [n]} s_i + 1) = O(M)$ requests in $U^{(t)}$. For each request i , to decide whether to add it or not in $U^{(t)}$, one has to check all inequalities at the completion times $p_j + o_j$ for $j \in S^{(t)} \cup U^{(t)}$ in Eq. (5). The number of inequalities we need to check is $O(M)$ since $|S^{(t)} \cup U^{(t)}| = O(M)$. Therefore, the feasibility check for each request i has a complexity of $O(M)$. Since we can add at most $O(M)$ number of requests to a batch, the complexity at time t is at most $O(M^2)$. \square

B.3 Proof of Theorem 4.3 in case of equal output length

We begin by computing the total end-to-end latency of MC-SF. Since all requests have identical prompt size and output length, each batch can accommodate at most $m = \lfloor \frac{M}{s+o} \rfloor$ requests. If M is not a multiple of $s + o$, Algorithm 1 may utilize some leftover memory to fit an additional request by carefully checking Equation (5). However, to upper bound the algorithm's latency, we assume a less efficient version of the algorithm: it always processes exactly m requests per batch, and any leftover memory capacity is wasted.

Let \mathcal{I}_n denote the input instance with n identical requests. W.L.O.G, we assume that $n > m$. Otherwise, the competitive ratio equals to 1 since all requests can be processed within a single batch. Take $n = km + p$, where $k \geq 1$ is some positive integer and $0 \leq p < m$ is a non-negative integer which is less than m . Processing all n requests requires $k + 1$ batches. The first k batches contain m requests in each, incurring a total latency of $mo \sum_{i=1}^k i$, and the final batch contains p requests, incurring a total latency of $po(k + 1)$. The total end-to-end latency is given by

$$\begin{aligned}
\text{TEL}(\mathcal{I}_n; \text{MC-SF}) &\leq \left(mo \sum_{i=1}^k i \right) + po(k + 1) \\
&= o \left(\frac{mk(k + 1)}{2} + p(k + 1) \right) \\
&= o \left(\frac{m}{2} \cdot \frac{n - p}{m} \cdot \frac{n + (m - p)}{m} + p \cdot \frac{n + (m - p)}{m} \right) \\
&= o \left(\frac{(n - p)(n + (m - p))}{2m} + \frac{p[n + (m - p)]}{m} \right) \\
&= \frac{o}{2m} \left(n^2 + nm + p(m - p) \right) \\
&\leq \frac{o}{2m} \left(n^2 + nm + \frac{m^2}{4} \right) \tag{14}
\end{aligned}$$

$$\begin{aligned}
&= \frac{on^2}{2m} + \frac{on}{2} + \frac{om}{8} \\
&\leq \frac{on^2}{2m} + \frac{on}{2} + \frac{on}{8} \tag{15} \\
&= \frac{on^2}{2m} + \frac{5on}{8},
\end{aligned}$$

where inequality (14) is due to $p(m - p)$ achieves its maximum when $p = m/2$. Inequality (15) is due to $n > m$.

Next, since $m = \left\lfloor \frac{M}{s+o} \right\rfloor \geq \frac{M}{s+o} - 1$, we further upper bound the total latency as follows:

$$\begin{aligned}
\text{TEL}(\mathcal{I}_n; \text{MC-SF}) &\leq \frac{on^2}{2m} + \frac{5on}{8} \\
&\leq \frac{on^2}{2} \frac{1}{\frac{M}{s+o} - 1} + \frac{5on}{8} \\
&= \frac{on^2}{2} \frac{s+o}{M} \left(\frac{1}{1 - \frac{s+o}{M}} \right) + \frac{5on}{8} \\
&\leq \frac{on^2}{2} \frac{s+o}{M} \left(1 + 2 \frac{s+o}{M} \right) + \frac{5on}{8} \tag{16}
\end{aligned}$$

$$\begin{aligned}
&= \frac{o(s+o)n^2}{2M} + \frac{o(s+o)^2n^2}{M^2} + \frac{5on}{8} \\
&\leq \frac{o(s+o)n^2}{2M} + \frac{o(s+o)n^2}{2M} + \frac{5on}{8} \tag{17} \\
&= \frac{o(s+o)n^2}{M} + \frac{5on}{8},
\end{aligned}$$

where inequality (16) is due to $\frac{s+o}{M} \leq \frac{1}{2}$, and the Taylor expansion has $\frac{1}{1-x} \leq 1 + 2x$ for any $0 \leq x \leq \frac{1}{2}$. Inequality (17) is also due to $\frac{s+o}{M} \leq \frac{1}{2}$.

Next, we derive a lower bound on $\text{OPT}(\mathcal{I}_n)$, the minimum total latency achievable by the hindsight optimal. As defined in Section 3, $\text{OPT}(\mathcal{I}_n)$ corresponds to the optimal objective value of the integer program given in Equation (1). We relax the integer constraint (4), which originally requires $x_{i,t} \in \{0, 1\}$ for all $i \in [n]$, $t \in [\bar{T}]$. We replace this with the linear relaxation $x_{i,t} \geq 0$. Note that we do not need to explicitly enforce $x_{i,t} \leq 1$, as constraint (2) ensures that each request is scheduled exactly once, and thus the total mass of $x_{i,t}$ over all t is 1. Let OPT-Primal denote the objective value of this relaxed linear program. The formulation is as follows:

$$\text{OPT-Primal} = \text{Minimize}_{x_{i,t}} \quad no + \sum_{i=1}^n \left(\sum_{t=0}^{\bar{T}} t \cdot x_{i,t} \right) \tag{18}$$

$$\text{subject to} \quad \sum_{t=0}^{\bar{T}} x_{i,t} = 1, \quad \forall i \in [n] \tag{19}$$

$$\sum_{i=1}^n \sum_{k=(t-o)^+}^{t-1} (s+t-k)x_{i,k} \leq M, \quad \forall t \in [\bar{T}] \tag{20}$$

$$x_{i,t} \geq 0, \quad \forall i \in [n], \forall t \in [\bar{T}] \tag{21}$$

It is straightforward to verify that $\text{OPT-Primal} \leq \text{OPT}(\mathcal{I}_n)$, since the feasible region of the relaxed linear program contains that of the original integer program. To analyze OPT-Primal , we now

derive its dual formulation, which we denote by OPT-Dual. The dual linear program is given by:

$$\text{OPT-Dual} = \text{Maximize}_{y_i, \lambda_t} \quad no + \sum_{i=1}^n y_i - M \sum_{t=1}^{\bar{T}} \lambda_t \quad (22)$$

$$\text{subject to} \quad y_i - \sum_{\tau=t+1}^{t+o} (s + \tau - t) \lambda_\tau \leq t, \quad \forall i \in [n], \forall t \in [\bar{T}] \quad (23)$$

$$\lambda_t \geq 0, \quad \forall t \in [\bar{T}] \quad (24)$$

By weak duality, we have $\text{OPT-Dual} \leq \text{OPT-Primal}$. Next, we construct a pair of feasible dual variables (\mathbf{y}, λ) and take the dual objective value as a further lower bound of OPT-Dual. We define:

$$y_i = \bar{y} = \left(\frac{(2s + o + 1)on}{2M} - \frac{(o - 1)(3s + 2o + 2)}{3(2s + o + 1)} \right)^+, \forall i \in [n] \quad (25)$$

$$\lambda_1 = \frac{2\bar{y} + \frac{2(o-1)(3s+2o+2)}{3(2s+o+1)}}{(2s + o + 1)o}, \quad (26)$$

$$\lambda_t = \left(\lambda_1 - \frac{2(t-1)}{(2s + o + 1)o} \right)^+, \forall t \in \{1, 2, \dots, \bar{T}\} \quad (27)$$

To check feasibility, constraint (24) is obvious since all λ_t are constructed as non-negative. The following lemma checks the constraint (23).

Lemma B.1. *By taking (\mathbf{y}, λ) as the vectors defined in Equations (25), (26), (27), constraint (23) is not violated.*

Proof of Lemma B.1. We prove by math induction. Base case: We first check the feasibility when $t = 0$. For any $i \in [n]$, we have

$$\begin{aligned} y_i - \sum_{\tau=1}^o (s + \tau) \lambda_\tau &= \bar{y} - (s + 1) \lambda_1 - \dots - (s + o) \lambda_o \\ &\leq \bar{y} - (s + 1) \lambda_1 - (s + 2) \left(\lambda_1 - \frac{2}{(2s + o + 1)o} \right) - \dots - (s + o) \left(\lambda_1 - \frac{2(o-1)}{(2s + o + 1)o} \right) \\ &= \bar{y} - \frac{(2s + o + 1)o}{2} \lambda_1 + s \frac{o(o-1)}{2} \frac{2}{(2s + o + 1)o} + \left(\frac{o(o+1)(2o+1)}{6} - \frac{o(o+1)}{2} \right) \frac{2}{(2s + o + 1)o} \\ &= \bar{y} - \frac{(2s + o + 1)o}{2} \lambda_1 + \frac{(o-1)(3s + 2o + 2)}{3(2s + o + 1)} \\ &= \bar{y} - \frac{(2s + o + 1)o}{2} \frac{2\bar{y} + \frac{2(o-1)(3s+2o+2)}{3(2s+o+1)}}{(2s + o + 1)o} + \frac{(o-1)(3s + 2o + 2)}{3(2s + o + 1)} \\ &= \bar{y} - \bar{y} - \frac{(o-1)(3s + 2o + 2)}{3(2s + o + 1)} + \frac{(o-1)(3s + 2o + 2)}{3(2s + o + 1)} = 0. \end{aligned}$$

Next, if the feasibility holds for t , that is, $\bar{y} - \sum_{\tau=t+1}^{t+o} (s + \tau - t)\lambda_\tau \leq t$, then we check whether the feasibility holds or not for $t + 1$. Observe that

$$\begin{aligned}
& \left(\bar{y} - \sum_{\tau=t+2}^{t+1+o} (s + \tau - (t + 1))\lambda_\tau \right) \\
&= \left(\bar{y} - \sum_{\tau=t+1}^{t+o} (s + \tau - t)\lambda_\tau \right) + \left((s + 1)\lambda_{t+1} + \sum_{\tau=t+2}^{t+o} \lambda_\tau - (s + o)\lambda_{t+1+o} \right) \\
&\leq t + \left((s + 1)\lambda_{t+1} + \sum_{\tau=t+2}^{t+o} \lambda_\tau - (s + o)\lambda_{t+1+o} \right) \\
&\leq t + \left((s + 1) \left(\lambda_1 - \frac{2t}{(2s + o + 1)o} \right) + \sum_{\tau=t+2}^{t+o} \left(\lambda_1 - \frac{2(\tau - 1)}{(2s + o + 1)o} \right) - (s + o) \left(\lambda_1 - \frac{2(t + o)}{(2s + o + 1)o} \right) \right) \\
&= t + (s + o)\lambda_1 - (s + o)\lambda_1 + \frac{2}{(2s + o + 1)o} \left((s + o)(t + o) - (s + 1)t - \sum_{\tau=t+2}^{t+o} (\tau - 1) \right) \\
&= t + \frac{2}{(2s + o + 1)o} \left((s + o)(t + o) - (s + 1)t - \frac{(2t + o)(o - 1)}{2} \right) \\
&= t + \frac{2}{(2s + o + 1)o} \left((st + so + ot + o^2) - (st + t) - \left(to - t + \frac{o^2}{2} - \frac{o}{2} \right) \right) \\
&= t + \frac{2}{(2s + o + 1)o} \left(so + \frac{o^2}{2} + \frac{o}{2} \right) \\
&= t + 1.
\end{aligned}$$

Therefore, we have the constraint (23) holds. \square

Next, we calculate the dual objective value:

$$no + \sum_{i=1}^n y_i - M \sum_{t=1}^{\bar{T}} \lambda_t \geq no + n\bar{y} - M \frac{\lambda_1(\lambda_1/(2/((2s + o + 1)o)))}{2},$$

The next lemma shows that the competitive ratio is upper bounded by 4.

Lemma B.2. *Under the choice of \bar{y} , λ_1 in Equations (25), (26), we have*

$$\frac{\frac{5on}{8} + \frac{o(s+o)n^2}{M}}{no + n\bar{y} - M \frac{\lambda_1(\lambda_1/(2/((2s+o+1)o)))}{2}} \leq 4,$$

for any s, o, n, M .

Proof of Lemma B.2. Let's first introduce some notations to shorten the equations. Denote $q = n/M$, $\beta = 2s + o + 1$, $\alpha = \frac{2(o-1)(3s+2o+2)}{3\beta}$. Then, we have

$$\bar{y} := \begin{cases} 0, & 0 < q < \frac{\alpha}{\beta o}, \\ \frac{q\beta o - \alpha}{2}, & q \geq \frac{\alpha}{\beta o}. \end{cases}$$

We can obtain

$$\frac{\frac{5on}{8} + \frac{o(s+o)n^2}{M}}{no + n\bar{y} - M \frac{\lambda_1(\lambda_1/(2/((2s+o+1)o))}{2}} = \frac{o(\frac{5}{8} + (s+o)q)}{o + \bar{y} - \frac{(2\bar{y} + \alpha)^2}{4q\beta o}}.$$

Next, we split the proof into two cases:

- *Case 1:* $0 < q < \frac{\alpha}{\beta o}$. In this case, we have the denominator equals to $o - \frac{\alpha^2}{4q\beta o}$. Further, we have

$$\begin{aligned} \alpha &= \frac{2(o-1)(3s+2o+2)}{3(2s+o+1)} \leq \frac{4}{3}o, \\ \frac{\alpha^2}{4q\beta o^2} &\leq \frac{4}{9} \cdot \frac{1}{q\beta} \leq \frac{4}{9} \cdot \frac{s+o}{2s+o+1} < \frac{4}{9}. \\ (s+o)q &\leq \frac{(s+o)\alpha}{\beta o} = \frac{2}{3} \frac{3s^2 + 5so + 5s + 2o^2 + 2o}{4s^2 + o^2 + 1 + 4so + 4s + 2o} \leq 4/3. \end{aligned}$$

Therefore, we have

$$\begin{aligned} \frac{o(\frac{5}{8} + (s+o)q)}{o + \bar{y} - \frac{(2\bar{y} + \alpha)^2}{4q\beta o}} &= \frac{\frac{5}{8} + (s+o)q}{1 - \frac{\alpha^2}{4q\beta o^2}} \\ &\leq \frac{\frac{5}{8} + \frac{4}{3}}{1 - \frac{4}{9}} = \frac{141}{40} < 4. \end{aligned}$$

- *Case 2:* $q > \frac{\alpha}{\beta o}$. Plug the expression of \bar{y} into $\frac{o(\frac{5}{8} + (s+o)q)}{o + \bar{y} - \frac{(2\bar{y} + \alpha)^2}{4q\beta o}}$, we have

$$\frac{o(\frac{5}{8} + (s+o)q)}{o + \bar{y} - \frac{(2\bar{y} + \alpha)^2}{4q\beta o}} = \frac{\frac{5}{8} + (s+o)q}{1 + \frac{q\beta}{4} - \frac{\alpha}{2o}}.$$

Observe that

$$\frac{\alpha}{2o} = \frac{1}{3} \frac{o-1}{o} \frac{3s+2o+2}{2s+o+1} \leq \frac{2}{3}.$$

Then, we have

$$\begin{aligned} 4 \left(1 + \frac{q\beta}{4} - \frac{\alpha}{2o} \right) &= 4 + q\beta - 4 \frac{\alpha}{2o} \\ &\geq 4 + q\beta - \frac{8}{3} \\ &= \frac{4}{3} + q\beta \\ &= \frac{4}{3} + q(2s+o+1) \\ &\geq \frac{5}{8} + q(s+o). \end{aligned}$$

□

Therefore, we have

$$\text{CR}(\mathcal{A}) = \frac{\text{TEL}(\mathcal{I}_n; \mathcal{A})}{\text{OPT}(\mathcal{I}_n)} \leq \frac{\text{TEL}(\mathcal{I}_n; \mathcal{A})}{\text{OPT-Dual}} \leq \frac{\frac{5on}{8} + \frac{o(s+o)n^2}{M}}{no + n\bar{y} - M \frac{\lambda_1(\lambda_1/(2/((2s+o+1)o))}{2}} \leq 4.$$

C Appendix for Section 5

All experiments were conducted on a Microsoft Surface Laptop with Snapdragon[®] X Elite (12 Core) processor.

Algorithm 2: Memory Constrained Benchmark (MC-Benchmark)

Input: Memory capacity M , time horizon T

Output: Schedule for processing requests

for each round $t = 1$ to T **do**

Let $S^{(t)}$ be the set of requests that have already stated processing, and let $R^{(t)}$ be the set of waiting requests at time t . Also set $U^{(t)} = \emptyset$

for each request $i \in R^{(t)}$ in ascending order of arrival time a_i **do**

Set a time list $t' = p_j + o_j$ for $j \in S^{(t)} \cup U^{(t)} \cup \{i\}$

if all inequalities in Equation (5) hold for all t' **then**

| Add request i to $U^{(t)}$

else

| Break the for loop

Process the requests in $S^{(t)} \cup U^{(t)}$

In this section, we provide additional details for the numerical experiments with real data. We take the memory capacity as 16,492 as observed in real experiments reported to us by systems engineers through private communication.

We next summarize the figures that support our key findings in the numerical experiments. Figure 5 displays the empirical distributions of input prompt lengths and output response lengths from the dataset used in our study. Figures 6 and 9 show that our algorithm consistently utilizes most of the available memory per batch, under both high-demand and low-demand conditions respectively. Figures 7 and 10 report the total latency for various values of the protection level parameter α , and identify recommended ranges for its selection in high- and low-demand scenarios, respectively. Finally, Figures 8 and 11 evaluate the impact of the KV cache clearing probability β on total latency, highlighting appropriate ranges of β for high- and low-demand settings respectively.

In Figure 7, we varied α while fixing $\beta = 0.1$ and $\beta = 0.2$. For both settings, $\alpha \in [0.15, 0.25]$ minimizes average latency. When $\alpha < 0.1$, performance degrades significantly as the protected memory is insufficient, necessitating frequent clearing and rescheduling of requests, which leads to redundant computation.

Figure 8 illustrates average latency for various values of β with fixed α values of 0.1 and 0.2. In both cases, the algorithm performs well with $\beta \in [0.05, 0.25]$. For extremely low β , the algorithm underperforms as insufficient clearing of requests limits memory availability. This may keep the

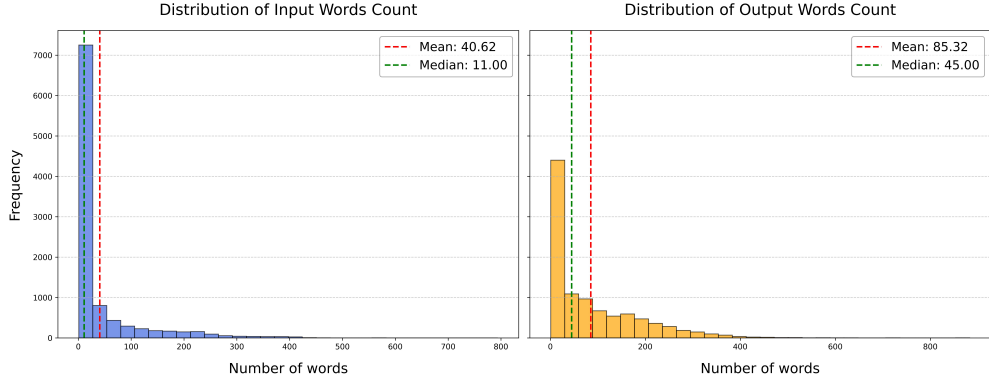


Figure 5: Distribution of the number of words of input prompt and output response respectively

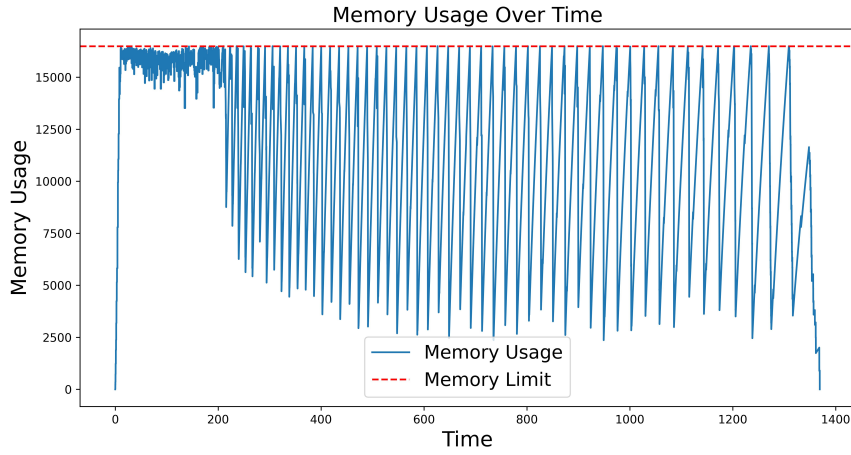


Figure 6: Memory Usage over Time for Algorithm 1 in the High Demand Case

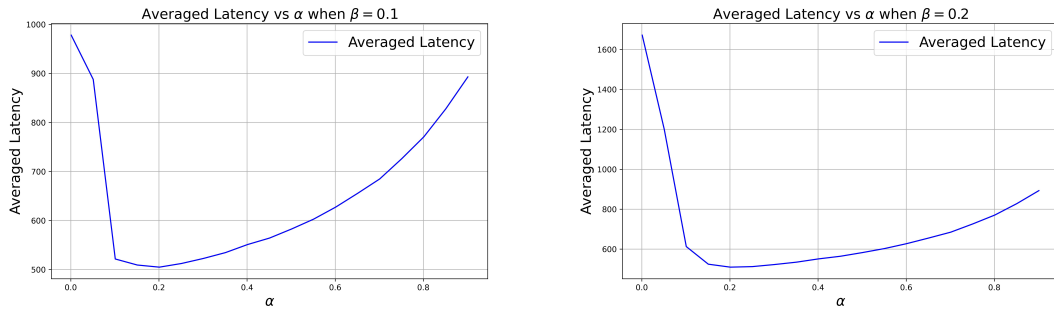


Figure 7: Average End-to-End Latency for Different α Values under the High Demand Case

memory usage be above the limit after clearing the processing requests. To clear enough memory with extremely small β , this requires a significant time. Conversely, higher β values are inefficient due to excessive request clearing, resulting in increased recomputation.

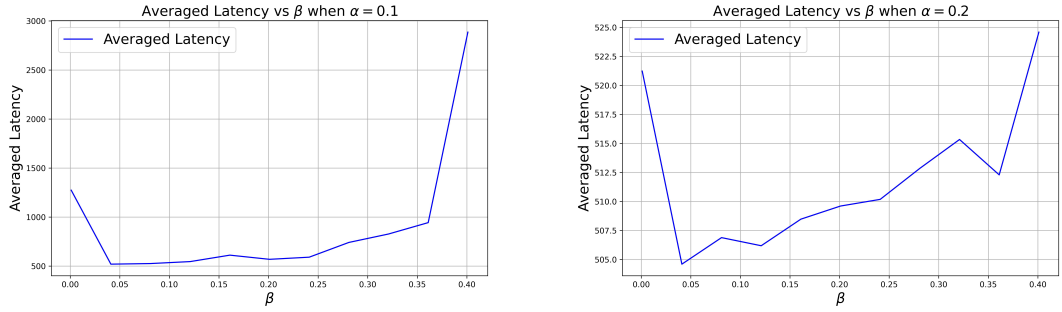


Figure 8: Average End-to-End Latency for Different β Values under the High Demand Case

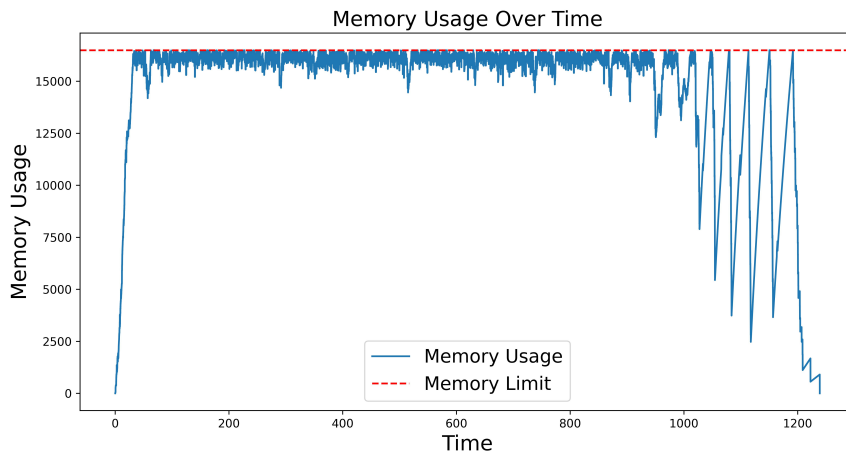


Figure 9: Memory Usage over Time for Algorithm 1 in the Low Demand Case

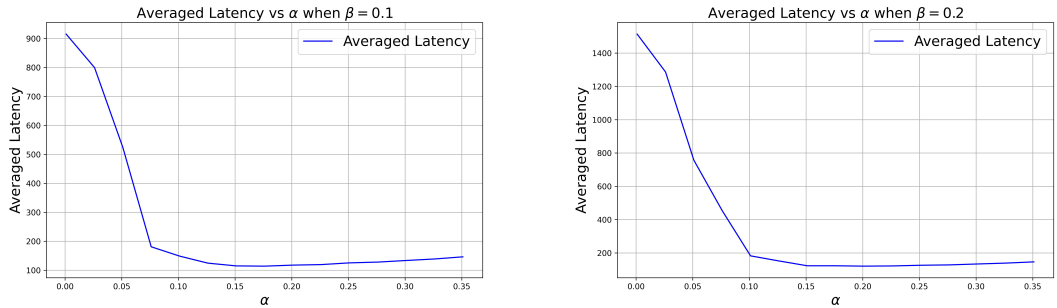


Figure 10: Average End-to-End Latency for Different α Values under the Low Demand Case

In Figure 10, we vary α while fixing β at 0.1 and 0.2. For both settings, values of α in the range $[0.10, 0.25]$ minimize average latency, while $\alpha < 0.1$ leads to significant performance degradation.

Figure 11 shows the average latency across various β values with α fixed at 0.1 and 0.2. In both

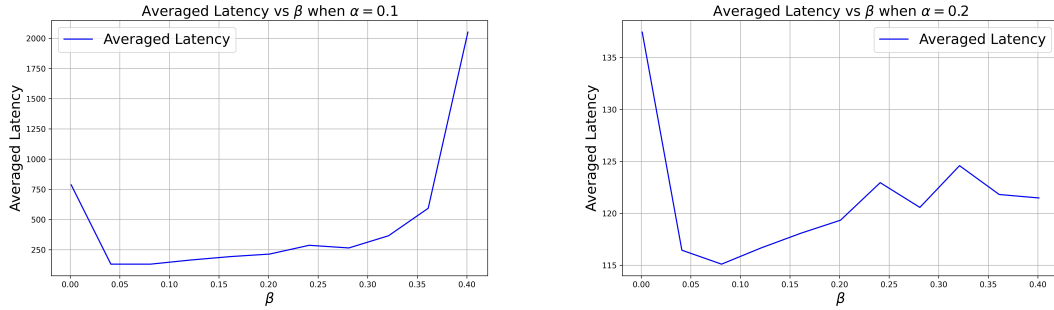


Figure 11: Average End-to-End Latency for Different β Values under the Low Demand Case

cases, the algorithm achieves stable performance for β values between 0.05 and 0.20. These trends are consistent with those observed in the high-demand scenario, indicating that similar parameter tuning benefits both models.

Finally, we provide a table with relevant statistics for the case of 1000 requests with arrival rate $\lambda = 50$ for 50 independent runs.

Table 1: Relevant statistics among 50 independent experiments of different algorithms where there are 1000 requests, and the arrival rate $\lambda = 50$

Algorithm	Average	Std. Dev.	Max	Min
MC-SF	32.112	0.354	33.097	31.505
MC-Benchmark	46.472	0.310	47.135	45.838
Benchmark $\alpha = 0.3$	51.933	0.324	52.532	51.204
Benchmark $\alpha = 0.25$	51.046	0.351	51.757	50.279
Benchmark $\alpha = 0.2, \beta = 0.2$	50.401	0.343	51.035	49.700
Benchmark $\alpha = 0.2, \beta = 0.1$	50.395	0.360	51.083	49.586
Benchmark $\alpha = 0.1, \beta = 0.2$	53.393	1.457	56.357	49.488
Benchmark $\alpha = 0.1, \beta = 0.1$	50.862	0.946	53.978	49.086